

Differential-geometrical approach to the dynamics of dissipationless incompressible Hall magnetohydrodynamics: II. Geodesic formulation and Riemannian curvature analysis of hydrodynamic and magnetohydrodynamic stabilities

ARAKI Keisuke

Faculty of Engineering, Okayama University of Science, 1-1 Ridai-cho, Kita-ku, Okayama 700-0005 JAPAN

E-mail: araki@are.ous.ac.jp

18 May 2022

Abstract. In this study, the dynamics of a dissipationless incompressible Hall magnetohydrodynamic (HMHD) medium are formulated as geodesics on a direct product of two volume-preserving diffeomorphism groups. Formulations are given for the geodesic and Jacobi equations based on a linear connection with physically desirable properties, which agrees with the Levi-Civita connection. Derivations of the explicit normal-mode expressions for the Riemannian metric, Levi-Civita connection, and related formulae and equations are also provided using the generalized Elsässer variables (GEVs). Examinations of the stabilities of the hydrodynamic (HD, $\alpha = 0$) and magnetohydrodynamic (MHD, $\alpha \rightarrow 0$) motions and the $O(\alpha)$ Hall-term effect in terms of the Jacobi equation and the Riemannian sectional curvature tensor are presented, where α represents the Hall-term strength parameter. It is very interesting that the sectional curvatures of the MHD and HMHD systems between two GEV modes were found to take both the positive (stable) and negative (unstable) values, while that of the HD system between two complex helical waves was observed to be negative definite. Moreover, for the MHD case, negative sectional curvatures were found to occur only when mode interaction was “local,” i.e., the wavenumber moduli of the main flow (say p) and perturbation (say k) were relatively close to each other. However, in the nonlocal limit ($k \ll p$ or $k \gg p$), the sectional curvatures were always positive. This result leads to the conjecture that the MHD interactions mainly excite wavy or non-growing motions; however, some local interactions cause dynamical instability that leads to chaotic or turbulent plasma motions. Additionally, it was found that the tendencies of the $O(\alpha)$ effects are opposite between the ion cyclotron and whistler modes.

1. Introduction

In the present study, we addressed the geodesic formulation and related stability problems of a dissipationless, incompressible Hall magnetohydrodynamic (HMHD)

system. The purposes of the study are twofold: to revisit the geodesic formulation framework from a physical viewpoint, and to apply it to the linear stability of the hydrodynamic (HD), magnetohydrodynamic (MHD), and HMHD systems, with a consideration of its applicability to the analysis of fully-developed homogeneous and isotropic turbulence.

Since Arnold cast the study of dynamical systems on Lie groups and related hydrodynamic topics in a unified form [1], multiple fluid dynamical systems have been recognized to exist on appropriate Lie groups [2]. The key to the Lagrangian formalism of Lie groups is the appropriate choice of the inner product and the Lie bracket, which are denoted hereafter by $\langle * | * \rangle$ and $[*, *]$, respectively. Once these two mathematical structures are defined, the variational formulation is formally established, and the evolution equation known as the Euler–Poincaré equation is derived [3].

However, the geodesic formulation, which was also discussed in [1], still seems to hold a somewhat bizarre position among the analytical mechanical theories of continuum mechanics because the Lagrangian or Hamiltonian mechanical descriptions of such systems work well without Riemannian geometrical notions such as the Levi–Civita connection and the Riemannian curvature tensor (e.g. [3]).

Despite this situation, the geodesic formulation perspective provides a powerful tool. The second variation of action, which yields the Jacobi equation, is known to provide information about the dynamical stabilities of the solutions ([4]; app. I). As an advantage, this approach provides a differential geometrical framework for the predictability problem of HD systems ([1]; §11). From this viewpoint, the attraction/repulsion (instability) or winding around (stability) of infinitesimally close paths is determined by the sign of the Riemannian curvature associated with the appropriate linear connection. The value of the sectional curvature is determined by the snapshot pair of a (possibly non-stationary) reference solution and a perturbation field imposed upon it without solving the evolution equation or eigenvalue problem.

Thus, geodesic formulation and the associated sectional curvature analysis have attracted much research interest. For example, Arnold [1] performed curvature analysis of the stability of the flow of a neutral incompressible fluid on a two-dimensional torus. These results were extended to three dimensions by Nakamura et al. [5] and to the general n -dimensional case by Lukatskii [6]. These researchers considered the sectional curvature between two Fourier modes and obtained negative values (i.e., instability of the basic flows). Ohkitani [7] approached the problem numerically, adopting the formulation by Rouchon [8] and solving the initial-value problem of the Jacobi equation. Zeitlin and Kambe [9] applied the method to the standard (or reduced single-fluid) system of MHD in two dimensions, and Hattori [10] later extended it to the n -dimensional case.

Moreover, as was reviewed by Vizman [11], a wide variety of dynamical systems, including Euler, ideal MHD, and Korteweg-de Vries (KdV) systems, have been formulated as geodesic equations on appropriate Lie groups. Despite the diversity of these dynamical systems, they did not include the geodesic equations on

semidirect products of two groups, also due to Vizman [12]. Recently, dissipationless, incompressible Hall MHD (HMHD) systems were found to be dynamical systems on the semidirect product of two volume-preserving diffeomorphisms, $S\text{Diff}(M) \times S\text{Diff}(M)$ [13]. Another interesting finding was that HMHD systems could also be formulated as dynamical systems on a direct product group, $S\text{Diff}(M) \times S\text{Diff}(M)$, by changing the basic variables [14].

Many dynamical systems has been treated in this framework, however, non-uniqueness problem of the definition of parallel translation seems scarcely discussed. A geodesic on a curved space (say $\gamma(t)$) is a curve such that its tangent vector $\dot{\gamma}$ is given by the parallel translation of itself along $\gamma(t)$. However, in a curved space, the ‘‘parallel translation’’ of a vector between two close points is determined by the *linear connection* around them and thus is not unique. In fact, it is known that when a linear connection (say Γ_{ij}^k) and an induced geodesic are given, the same geodesic is given by the connection generated by the linear combination $\Gamma_{ij}^{*k} = t\Gamma_{ij}^k + (1-t)\Gamma_{ji}^k$, where the parameter t is related to the *torsion* associated with Γ^* ([15]; ch. III, §7). This non-uniqueness of the connections implies that the ensemble of the curves determined by the Euler–Lagrange equation associated with a certain variational problem does not define the corresponding linear connection uniquely. Thus, it is necessary to consider the physically appropriate linear connection, despite the torsion-free condition ($\Gamma_{ij}^k = \Gamma_{ji}^k$) often being imposed explicitly or assumed implicitly.

HMHD was firstly derived by Lighthill [16] and is based on the following approximations: the MHD approximation of the Lorentz force by the electron component of the plasma ($\mathbf{E} + \mathbf{V}_e \times \mathbf{B} = \mathbf{0}$); and the approximation of the current density field generated by the difference between the ion and electron fluid motions ($\mathbf{V}_i - \mathbf{V}_e = \alpha \mathbf{J}/en_e$); and an approximate form of Ampere’s law ($\nabla \times \mathbf{B} = \mu_0 \mathbf{J}$). The basic equations are as follows:

$$\begin{aligned} \nabla \cdot \mathbf{u} &= \nabla \cdot \mathbf{b} = 0, \\ \partial_t \mathbf{u} &= \mathbf{u} \times \boldsymbol{\omega} + \mathbf{j} \times \mathbf{b} - \nabla P, \\ \partial_t \mathbf{b} &= \nabla \times (\mathbf{u} \times \mathbf{b}) - \alpha \nabla \times (\mathbf{j} \times \mathbf{b}), \end{aligned} \tag{1}$$

where \mathbf{u} , \mathbf{b} , $\boldsymbol{\omega}$, \mathbf{j} , P , and α are the appropriately nondimensionalized variables corresponding to the ion velocity, magnetic field, vorticity ($\boldsymbol{\omega} = \nabla \times \mathbf{u}$), current density ($\mathbf{j} = \nabla \times \mathbf{b}$), generalized pressure, and Hall-term strength parameter, respectively.

As for the stability problems of the HMHD system, since Holm’s pioneering work in this field [17], the analytical mechanical approaches have been mainly carried out from the Hamiltonian mechanical viewpoint (e.g. [18, 19, 20]). The energy-Casimir method was one of the principal tools for the stability analysis (e.g. [3]; §1.7). The method treats only the stability of the *stationary solutions*, though the analysis result states the Lyapunov stability, i.e., a priori estimation of perturbation amplitude for a sufficiently long time interval. In the present study, since both the energy-Casimir method and the Riemannian curvature analysis are based on the second variation of some appropriate

functional, we will discuss their conceptual correspondence.

As for the fully-developed turbulence of the HMHD systems, the effects of the Hall term on the properties of MHD turbulence have been attracted interests of many researchers from various viewpoints including the closure approach in the weak/wave turbulence framework [21], evaluation of turbulent energy transfer and dynamo action using direct numerical simulation (DNS) data [22], and coherent structure formation by DNS [23].

In the present study, in order to evaluate characteristic time of turbulent flows, we will attempt to apply the Riemannian curvature analysis to the turbulence problem under the the statistical homogeneity and isotropy assumption. Estimation of characteristic time scale (for example, Lyapunov exponent) has been recognized as one of the important issues of chaos and turbulence theories [24]. As will be seen in the deriving process and interpretation of its implication in section 3, the sectional curvature operator will be shown to indicates the characteristic time of perturbation growth, since it has dimension of the reciprocal of the square of time [T^{-2}]. We utilize here the important advantage of geodesic approach that the Riemannian curvature is computable for non-stationary solutions.

As for the normal-mode analysis, it should be remarked that application of the geometrical method to the dissipationless, incompressible HD, MHD, and HMHD systems has its foundation on the following fact: these three systems were found to have common dynamical system features [25]; that is, each system has its own action-preserving integro-differential operator, and the corresponding eigenfunctions yield formally the same spectral representation as that of the related formulae and equations. In particular, we found that the product of the Riemannian metric g_{ij} with the structure constants C_{jk}^i of the Lie group was given by the product of the eigenvalue $\Lambda(i)$ of the operator with a certain totally antisymmetric tensor T_{ijk} : $g_{i\alpha}C_{jk}^\alpha = \Lambda(i)T_{ijk}$.

The eigenfunctions in the HMHD system are generally given by double Beltrami flows (DBFs), namely, force-free stationary solutions for a two-fluid plasma, as determined by Mahajan and Yoshida [26]. Among the DBFs, considering the influence of a uniform background magnetic field and the Hall-term effect vanishing limit, the generalized Elsässer variables (GEVs [21]) have been found to be the most suitable for avoiding problems with singularities in the standard MHD limit [14].

This paper is organized as follows. In section 2, the mathematical preliminaries for the geodesic formulation of the HMHD system are reviewed. In section 3, the formulation of the linear stability problem as the Jacobi equation and the derivation of the Riemannian metric tensor are presented. Stability analyses of the HD, MHD, and lowest-order of the Hall-term effect are provided in section 4. A discussion is given in section 5.

2. Geodesic formulation of a dissipationless, incompressible HMHD system

In this section, we review some mathematical preliminaries of the geodesic formulation of a dissipationless, incompressible HMHD system. First, the derivation of the equation of motion of an incompressible HMHD fluid from Hamilton's principle is presented as a review of the Lagrangian mechanical foundation. Next, the connection that causes the geodesic equation to agree with the equation of motion is discussed.

2.1. Lagrangian mechanical foundations of a dissipationless, incompressible HMHD system

The details of the mathematical backgrounds were described in [13, 14, 25]. In this section, we introduce some mathematical notions and notation which was not explained in the previous studies but will use in the following sections.

As is mentioned in the section 1, the key mathematical structures are the Riemannian metric and the Lie bracket. For the HMHD systems, they are defined as follows [14]:

$$\langle \vec{\mathbf{V}}_1 | \vec{\mathbf{V}}_2 \rangle := \int d^3\vec{x} \left[\mathbf{V}_{i1} \cdot \mathbf{V}_{i2} + \alpha^{-2} (\nabla \times)^{-1} (\mathbf{V}_{i1} - \mathbf{V}_{e1}) \cdot (\nabla \times)^{-1} (\mathbf{V}_{i2} - \mathbf{V}_{e2}) \right], \quad (2)$$

$$[\vec{\mathbf{V}}_1, \vec{\mathbf{V}}_2] := \left(\nabla \times (\mathbf{V}_{i1} \times \mathbf{V}_{i2}), \nabla \times (\mathbf{V}_{e1} \times \mathbf{V}_{e2}) \right), \quad (3)$$

where $\nabla \times$ and $(\nabla \times)^{-1}$ are the curl operator and its inverse[‡], and the *generalized velocity*, $\vec{\mathbf{V}} = (\mathbf{V}_i, \mathbf{V}_e)$ [§], is the pair of the ion and electron velocity fields, which are related to the variables used in Eq. (1) by

$$\mathbf{u} = \mathbf{V}_i, \quad \boldsymbol{\omega} = \nabla \times \mathbf{V}_i, \quad \mathbf{j} = \alpha^{-1} (\mathbf{V}_i - \mathbf{V}_e), \quad \mathbf{b} = \alpha^{-1} (\nabla \times)^{-1} (\mathbf{V}_i - \mathbf{V}_e). \quad (4)$$

Using these variables, the combination of these mathematical structures reads as

$$\langle \vec{\mathbf{V}}_3 | [\vec{\mathbf{V}}_1, \vec{\mathbf{V}}_2] \rangle = \int d^3\vec{x} \left[\boldsymbol{\omega}_3 \cdot (\mathbf{u}_1 \times \mathbf{u}_2) + \mathbf{b}_3 \cdot (\mathbf{u}_1 \times \mathbf{j}_2 + \mathbf{j}_1 \times \mathbf{u}_2 - \alpha \mathbf{j}_1 \times \mathbf{j}_2) \right]. \quad (5)$$

The term $\vec{\mathbf{V}}$ -variable indicates the elements of the function space of the ion and electron velocity-field pairs.

Note that, when $\alpha = 0$, the second term of the inner product Eq. (2), which gives the magnetic energy in physical context, vanishes, because the difference between the ion and electron fluids is exactly zero ($\mathbf{V}_i - \mathbf{V}_e = 0$). Thus, the system describes the HD one (see Appendix 5). In the $\alpha \rightarrow 0$ limit, however, the term remains at $O(1)$ in amplitude and the system is reduced to the MHD one.

[‡] Here we use the relation $\nabla \times (\mathbf{a} \times \mathbf{b}) = (b^k \partial_k a^i - a^k \partial_k b^i) \partial_i$ that holds when \mathbf{a} and \mathbf{b} are divergence-free. The sign of the Lie bracket is chosen to satisfy the Hausdorff formula $e^{\boldsymbol{\xi}} e^{\boldsymbol{\eta}} = \exp(\boldsymbol{\xi} + \boldsymbol{\eta} + \frac{1}{2} [\boldsymbol{\xi}, \boldsymbol{\eta}] + \dots)$, where e and \exp denote the exponential map of a vector field (i.e. $\exp(t\mathbf{V})$ is a solution of the PDE $\partial_t \vec{\mathbf{X}} = \mathbf{V}$ for a fixed \mathbf{V}).

[§] In this paper, an arrow above a symbol denotes its multifunctional character. For example, a position vector is expressed by $\vec{x} = (x^1, x^2, x^3)$, and a pair of vector fields by $\vec{\mathbf{V}} = (\mathbf{V}_i, \mathbf{V}_e)$. Boldface letters are used to denote vector fields on M .

The *Lie derivatives* are defined as the “advectations” of functions, vector fields, and tensor fields. They provide tools for proving certain conservation laws associated with the Lagrangian invariants [27, 28]. The Lie derivative of the vector fields on the configuration space (say G) is defined by an extension of the basic definition (e.g., [15]; ch. I, §3) to the direct product group:

$$\vec{L}_{\vec{V}}\vec{\xi} = \lim_{t \rightarrow 0} \frac{\vec{\xi} - \phi^*(t)\vec{\xi}}{t} = \lim_{s \rightarrow 0} \lim_{t \rightarrow 0} \frac{\psi(s) - \phi(t) \circ \psi(s) \circ (\phi(t))^{-1}}{st} = [\vec{\xi}, \vec{V}],$$

where $\psi(s)$ and $\phi(t)$ are the one-parameter subgroups of G that satisfy $\psi(0) = \phi(0) = e$, $\vec{\xi} := \partial_s \psi(s)|_{s=0}$, and $\vec{V} = \partial_t \phi(t)|_{t=0}$.

The action S is defined along a path $\gamma(t; \epsilon) \subset G$, where t and ϵ are a line parameter and a small parameter for variation, respectively. Using the generalized velocities $\vec{V} = (\mathbf{V}_i(t), \mathbf{V}_e(t))$ and the fluid particle displacement fields $\vec{\xi} = (\xi_i(t), \xi_e(t))$, the path γ can be approximated locally by

$$\gamma(t + \tau; 0) \approx \bar{e}^{\tau \vec{V}(t)} \circ \gamma(t; 0), \quad \gamma(t; \epsilon) \approx \bar{e}^{\epsilon \vec{\xi}(t)} \circ \gamma(t; 0),$$

where $\bar{e}^{\tau \vec{V}(t)} = (e^{\tau \mathbf{V}_i(t)}, e^{\tau \mathbf{V}_e(t)})$, $\bar{e}^{\epsilon \vec{\xi}(t)} = (e^{\epsilon \xi_i(t)}, e^{\epsilon \xi_e(t)})$. Let $\vec{V}_\epsilon = \vec{V} + \epsilon \vec{v}$ be the tangent vector of $\gamma(t; \epsilon)$. The perturbation, \vec{v} , is related to the variation of path $\vec{\xi} = (\xi_i, \xi_e)$ by *Lin constraints* [3]

$$\vec{v} = \partial_t \vec{\xi} + [\vec{\xi}, \vec{V}] = (\partial_t + \vec{L}_{\vec{V}})\vec{\xi}, \quad (6)$$

which corresponds to the $O(\epsilon\tau)$ terms of the asymptotic relation

$$\bar{e}^{\tau \vec{V}_\epsilon(t)} \approx \bar{e}^{\epsilon \vec{\xi}(t+\tau)} \circ \bar{e}^{\tau \vec{V}(t)} \circ \bar{e}^{-\epsilon \vec{\xi}(t)},$$

(e.g., [14]; app. A). The value of the action on the path $\{\gamma(t; \epsilon)\}$ is $S_\epsilon = \frac{1}{2} \int_0^1 \langle \vec{V}_\epsilon | \vec{V}_\epsilon \rangle dt$. Its first variation becomes

$$\begin{aligned} \left. \frac{\partial S_\epsilon}{\partial \epsilon} \right|_{\epsilon=0} &= \int_0^1 dt \langle \vec{V} | \dot{\vec{\xi}} + \vec{L}_{\vec{V}} \vec{\xi} \rangle \\ &= \langle \vec{V} | \vec{\xi} \rangle \Big|_{t=0}^{t=1} - \int_0^1 dt \langle \dot{\vec{V}} | \vec{\xi} \rangle + \int_0^1 dt \langle \vec{L}_{\vec{V}}^\dagger \vec{V} | \vec{\xi} \rangle, \end{aligned} \quad (7)$$

where the adjoint operator \vec{L}^\dagger is defined by||

$$\langle \vec{L}_{\vec{V}_1}^\dagger \vec{V}_2 | \vec{V}_3 \rangle := \langle \vec{V}_2 | \vec{L}_{\vec{V}_1} \vec{V}_3 \rangle = \langle \vec{V}_2 | [\vec{V}_3, \vec{V}_1] \rangle \quad (8)$$

$$= \int d^3 \vec{x} \left\{ \mathbf{u}_3 \cdot (\mathbf{u}_1 \times \boldsymbol{\omega}_2 + \mathbf{j}_1 \times \mathbf{b}_2) + \mathbf{b}_3 \cdot \nabla \times [(\mathbf{u}_1 - \alpha \mathbf{j}_1) \times \mathbf{b}_2] \right\}. \quad (9)$$

Equation (9) yields the following explicit expression of the operator \vec{L}^\dagger :

$$(\vec{L}_{\vec{V}_1}^\dagger \vec{V}_2)_i = \left(\mathbf{V}_{i1} \times (\nabla \times \mathbf{V}_{i2}) + \alpha^{-2} (\mathbf{V}_{i1} - \mathbf{V}_{e1}) \times (\nabla \times)^{-1} (\mathbf{V}_{i2} - \mathbf{V}_{e2}) \right)_S, \quad (10)$$

$$(\vec{L}_{\vec{V}_1}^\dagger \vec{V}_2)_i - (\vec{L}_{\vec{V}_1}^\dagger \vec{V}_2)_e = (\nabla \times)^2 \left(\mathbf{V}_{e1} \times (\nabla \times)^{-1} (\mathbf{V}_{i2} - \mathbf{V}_{e2}) \right). \quad (11)$$

|| Note that the adjoint operator \vec{L}^\dagger is denoted by $B(*, *)$ in Arnold's work [1, 2, 4].

Hereafter $(*)_S$ denotes the solenoidal component of vector field obtained by Hodge decomposition (e.g., [29]; §2.10). Thus, Hamilton's principle yields the following Euler–Lagrange equation:

$$\dot{\vec{V}} = \vec{L}_{\vec{V}}^\dagger \vec{V}, \quad (12)$$

which is the well-known *Euler–Poincaré equation* ([3]; ch. 13). Application of Equation (9) to this equation derives Eq. (1).

2.2. Linear connection with physically desirable properties

As was discussed in the section 1, the Euler–Lagrange equation derived in the previous section does not determine the parallel translation of a vector uniquely. Thus, we present here the derivation of a linear connection on \vec{V} -variable space $\tilde{\nabla}$ that satisfies physically desirable features.

To begin with, we postulate that the connection is defined by a combination of the Riemannian metric and Lie bracket:

$$\langle \vec{V}_3 | \tilde{\nabla}_{\vec{V}_1} \vec{V}_2 \rangle := C_1 \langle \vec{V}_3 | [\vec{V}_1, \vec{V}_2] \rangle + C_2 \langle \vec{V}_1 | [\vec{V}_2, \vec{V}_3] \rangle + C_3 \langle \vec{V}_2 | [\vec{V}_3, \vec{V}_1] \rangle, \quad (13)$$

where C_i are constants. This postulate leads to the expression of $\tilde{\nabla}$ in terms of the Lie derivative L and its adjoint \vec{L}^\dagger as

$$\tilde{\nabla}_{\vec{V}_1} \vec{V}_2 = C_1 \vec{L}_{\vec{V}_2} \vec{V}_1 - C_2 \vec{L}_{\vec{V}_2}^\dagger \vec{V}_1 + C_3 \vec{L}_{\vec{V}_1}^\dagger \vec{V}_2. \quad (14)$$

C_i are determined by the following three physical conditions.

(i) *The connection $\tilde{\nabla}$ is metric-preserving:*

$$\tilde{\nabla}_{\vec{V}_3} \langle \vec{V}_1 | \vec{V}_2 \rangle = \langle \tilde{\nabla}_{\vec{V}_3} \vec{V}_1 | \vec{V}_2 \rangle + \langle \vec{V}_1 | \tilde{\nabla}_{\vec{V}_3} \vec{V}_2 \rangle = 0. \quad (15)$$

Mathematically, this relation simply reflects the right-invariance of the Riemannian metric. In a physical context, however, this condition guarantees not only energy conservation as a whole, but also the *detailed energy balance* between the interacting modes. This condition leads to the relation $C_1 = C_3$.

(ii) *The Euler–Lagrange Equation (12) agrees with the geodesic equation under the connection $\tilde{\nabla}$: $\tilde{\nabla}_{\vec{V}} \vec{V} = -\vec{L}_{\vec{V}}^\dagger \vec{V}$.* The relation $C_2 - C_3 = 1$ is derived here.

(iii) *The substantial derivative $\partial_t + \tilde{\nabla}_{\vec{V}}$ is covariant against the Galilean boost for arbitrary frozen-in vector fields.* The calculation is given in Appendix 1, and results in $C_1 + C_3 = -1$.

These three conditions uniquely determine the coefficients to be $C_1 = -C_2 = C_3 = -1/2$. The connection that satisfies these conditions is given by

$$\tilde{\nabla}_{\vec{V}_1} \vec{V}_2 = -\frac{1}{2} \vec{L}_{\vec{V}_2} \vec{V}_1 - \frac{1}{2} \vec{L}_{\vec{V}_1}^\dagger \vec{V}_2 - \frac{1}{2} \vec{L}_{\vec{V}_2}^\dagger \vec{V}_1. \quad (16)$$

Substituting Equations (5) and (9), we can obtain the combination of the Riemannian metric and the following physically desirable connection:

$$\begin{aligned} \langle \vec{V}_3 | \tilde{\nabla}_{\vec{V}_1} \vec{V}_2 \rangle &= \frac{1}{2} \int d^3\vec{x} \left\{ \mathbf{v}_3 \cdot \left[\boldsymbol{\omega}_1 \times \mathbf{v}_2 - \mathbf{v}_1 \times \boldsymbol{\omega}_2 - \nabla \times (\mathbf{v}_1 \times \mathbf{v}_2) + \mathbf{b}_1 \times \mathbf{j}_2 - \mathbf{j}_1 \times \mathbf{b}_2 \right] \right. \\ &\quad \left. + \mathbf{b}_3 \cdot \left[\nabla \times [\mathbf{b}_1 \times (\mathbf{v}_2 - \alpha \mathbf{j}_2) - (\mathbf{v}_1 - \alpha \mathbf{j}_1) \times \mathbf{b}_2] - \mathbf{v}_1 \times \mathbf{j}_2 - \mathbf{j}_1 \times \mathbf{v}_2 + \alpha \mathbf{j}_1 \times \mathbf{j}_2 \right] \right\}. \quad (17) \end{aligned}$$

Note that this connection satisfies the torsion-free condition

$$[\vec{\mathbf{V}}_1, \vec{\mathbf{V}}_2] = \tilde{\nabla}_{\vec{\mathbf{v}}_2} \vec{\mathbf{V}}_1 - \tilde{\nabla}_{\vec{\mathbf{v}}_1} \vec{\mathbf{V}}_2, \quad (18)$$

i.e., it is the Levi–Civita connection on G associated with the Riemannian metric (2). Conversely, the torsion-free condition itself requires $2C_1 = -1$ and $C_2 + C_3 = 0$ and it can surrogate the physical conditions (ii) and (iii).

3. Linear stability analysis in the geodesic formulation

3.1. Formulation of the linear stability analysis and a remark on its applicability

In this section, we discuss the linear stability problem in the geodesic-formulation framework. As is well known, the second variation of the curve length yields the Jacobi equation.

Let $\vec{\mathbf{V}}$ be a “reference” solution that satisfies the equation of motion (12):

$$\frac{\mathrm{D}}{\mathrm{D}t} \vec{\mathbf{V}} = 0, \quad (19)$$

where $\frac{\mathrm{D}}{\mathrm{D}t} := \frac{\partial}{\partial t} + \tilde{\nabla}_{\vec{\mathbf{v}}}$ is the “substantial derivative” with respect to the Levi–Civita connection (16). The linear stability of the reference solution $\vec{\mathbf{V}}$ is determined by the evolution equation

$$\frac{\mathrm{D}}{\mathrm{D}t} \vec{\mathbf{v}} + \tilde{\nabla}_{\vec{\mathbf{v}}} \vec{\mathbf{V}} = 0, \quad (20)$$

where $\vec{\mathbf{v}}$ is a small perturbation of $\vec{\mathbf{V}}$. Remember that the Jacobi field $\vec{\xi}$ and the perturbation $\vec{\mathbf{v}}$ are closely related by Lin constraints (6):

$$\vec{\mathbf{v}} = \frac{\mathrm{D}}{\mathrm{D}t} \vec{\xi} - \tilde{\nabla}_{\vec{\xi}} \vec{\mathbf{V}}, \quad (21)$$

where the torsion-free condition (18) has been used. Substituting the Lin constraints (21) into the perturbation Equation (20) and using Equations (19) and (21), we can eliminate $\vec{\mathbf{v}}$ and obtain the following evolution equation for $\vec{\xi}$:

$$\left(\frac{\mathrm{D}}{\mathrm{D}t} \right)^2 \vec{\xi} + R(\vec{\xi}, \vec{\mathbf{V}}) \vec{\mathbf{V}} = 0 \quad (22)$$

where R is the Riemannian curvature tensor given by

$$R(\vec{\xi}, \vec{\mathbf{V}}) = \tilde{\nabla}_{\vec{\xi}} \tilde{\nabla}_{\vec{\mathbf{V}}} - \tilde{\nabla}_{\vec{\mathbf{V}}} \tilde{\nabla}_{\vec{\xi}} - \tilde{\nabla}_{\vec{\xi}} \tilde{\nabla}_{\vec{\mathbf{V}}} + \tilde{\nabla}_{\vec{\mathbf{V}}} \tilde{\nabla}_{\vec{\xi}} \quad (23)$$

[15]. This is the Jacobi equation associated with the reference solution $\vec{\mathbf{V}}$. It is convenient to rewrite this equation as a first order simultaneous differential equations as follows:

$$\frac{\mathrm{D}}{\mathrm{D}t} \begin{pmatrix} \vec{\xi} \\ \vec{\eta} \end{pmatrix} = \begin{pmatrix} O & I \\ -R'(\vec{\mathbf{V}}, \vec{\mathbf{V}}) & O \end{pmatrix} \begin{pmatrix} \vec{\xi} \\ \vec{\eta} \end{pmatrix}, \quad (24)$$

where $\vec{\eta} := \frac{\mathrm{D}}{\mathrm{D}t} \vec{\xi}$ and the multilinear operator R' is defined by $R'(\vec{\mathbf{V}}, \vec{\mathbf{V}}) \vec{\xi} := R(\vec{\xi}, \vec{\mathbf{V}}) \vec{\mathbf{V}}$.

Note that, since the PDE (24) requires a pair of $\vec{\mathbf{V}}$ -variables, $\vec{\xi}$ and $\vec{\eta}$, as an initial condition, by setting them appropriately, one can treat somewhat wider classes of stability problems than those commented in Arnold’s textbook [4] (see Appendix 2).

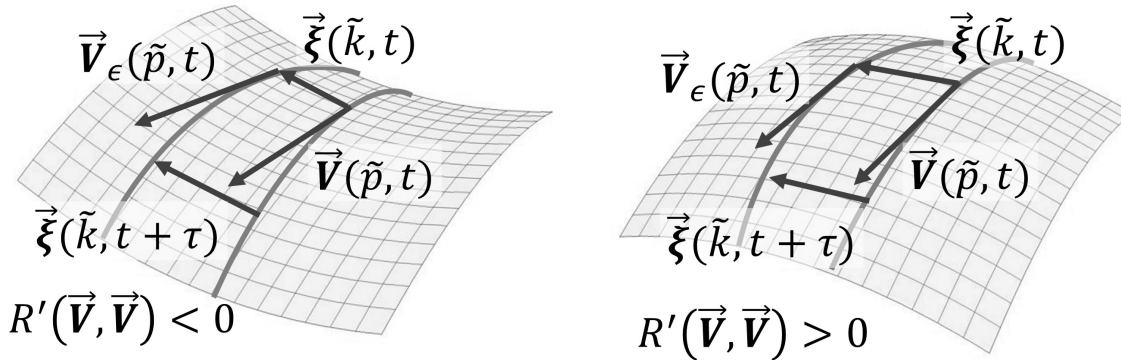


Figure 1. Illustration of the implication of the Riemannian curvature analysis. The pictures represent two dimensional surfaces locally spanned by the family of the solution paths $\gamma(t; \epsilon)$, where t and ϵ are the time and perturbation parameters. Differentiations with respect to t and ϵ give the generalized velocity $\vec{V}_\epsilon(t) = \dot{\gamma}(t; \epsilon)$ and the perturbation field $\vec{\xi}(t) = \partial_\epsilon \gamma(t; \epsilon)$, respectively. When the curvature is negative (left), there is a perturbation field that grows exponentially, and thus, the solution paths separate each other gradually as time goes by. When the curvature is positive (right), the norm of perturbation field does not grow, and thus, the solution paths remain close each other.

Physical implication of the Riemannian curvature: Temporal behaviors of $\vec{\xi}$ and $\vec{\eta}$ are determined by the eigenvalues (say Λ) of the eigenequation of the matrix operator in Equation (24),

$$\Lambda^2 I + R'(\vec{V}, \vec{V}) = 0.$$

If the curvature term is *negative*, the eigenvalues are real and the norm of the solution grows exponentially. However, when the curvature term is *positive*, the eigenvalues are purely imaginary, i.e., the solution is expected to be oscillatory (cf. [4]; app. 1, §I). In Figure 1, we present the schematic picture of the implications of sectional curvature.

Since dimension of the eigenvalue Λ is reciprocal of time, square root of the moduli of the Riemannian curvature indicate characteristic time scale of the disturbance fields. Thus, the large moduli of the curvature implies the rapid temporal variations irrespective of oscillatory or growing.

Note that, since the Riemannian curvature is defined by the covariant derivatives, the result describes the behaviour of solution paths for a very short time interval in general. Thus, one should be very careful to interpret the results, though applicability to predictability problems has been claimed. Despite this shortcoming, the Riemannian curvature analysis has a powerful advantage that it can be calculated for arbitrary snapshot pair of (possibly non-stationary) reference solution and perturbation without solving the evolution equation or eigenvalue problem.

3.2. Normal mode representation of the Jacobi equation and the Riemannian curvature tensor

We describe here the time evolution of the norm of solutions to Equation (24) that is defined by $\|\vec{\xi}\|^2 := \langle \vec{\xi} | \vec{\xi} \rangle + \langle \vec{\eta} | \vec{\eta} \rangle$. Taking the inner product of Equation (24) with $(\vec{\xi} \ \vec{\eta})$ and using the metric preserving property of the Levi-Civita connection (15), $\langle \vec{\xi} | \nabla_{\vec{v}} \vec{\xi} \rangle = \langle \vec{\eta} | \nabla_{\vec{v}} \vec{\eta} \rangle = 0$, we can obtain the following time evolution of the norm of the Jacobi field:

$$\frac{1}{2} \frac{d}{dt} \left(\langle \vec{\xi} | \vec{\xi} \rangle + \langle \vec{\eta} | \vec{\eta} \rangle \right) = \langle \vec{\xi} | \vec{\eta} \rangle - \langle \vec{\eta} | R(\vec{\xi}, \vec{V}) \vec{V} \rangle. \quad (25)$$

Substituting the normal mode expansions of \vec{V} -variables, e.g. $\vec{V} = \sum_{\tilde{k}} \widehat{V}(\tilde{k}; t) \vec{\Phi}(\tilde{k}; \vec{x})$, where $\vec{\Phi}$ is the GEV given by (55), we obtain the GEV representation of the equation as

$$\begin{aligned} \frac{1}{2} \frac{\partial}{\partial t} \left(|\widehat{\xi}(\tilde{k}; t)|^2 + |\widehat{\eta}(\tilde{k}; t)|^2 \right) &= \overline{\widehat{\xi}(\tilde{k}; t)} \widehat{\eta}(\tilde{k}; t) \\ &- g(\tilde{k})^{-1} \sum_{\tilde{p}} \sum_{\tilde{q}} \sum_{\tilde{r}}^{\tilde{k}=\tilde{p}+\tilde{q}+\tilde{r}} \left\langle \overline{\vec{\Phi}(\tilde{k})} \middle| R(\vec{\Phi}(\tilde{p}), \vec{\Phi}(\tilde{q})) \vec{\Phi}(\tilde{r}) \right\rangle \widehat{V}(\tilde{q}; t) \widehat{V}(\tilde{r}; t) \widehat{\xi}(\tilde{p}; t) \overline{\widehat{\eta}(\tilde{k}; t)} \end{aligned} \quad (26)$$

for each mode. Hereafter, the tilde notation \tilde{k} stands for the set of wavenumber, helicity, and linear-mode-branch index, $(\tilde{k}, \sigma_k, s_k)$, overbar denotes complex conjugate, and $g(\tilde{k}) := \langle \vec{\Phi}(\tilde{k}) | \vec{\Phi}(\tilde{k}) \rangle$ is the value of the Riemannian metric for mode \tilde{k} . The component of the Riemannian curvature tensor for the GEV modes is given by

$$\begin{aligned} &g(\tilde{k})^{-1} \left\langle \overline{\vec{\Phi}(\tilde{k})} \middle| R(\vec{\Phi}(\tilde{p}), \vec{\Phi}(\tilde{q})) \vec{\Phi}(\tilde{r}) \right\rangle \\ &= g(\tilde{k})^{-1} \left\langle \vec{\Phi}(-\tilde{k}) \middle| \widetilde{\nabla}_{\vec{\Phi}(\tilde{p})} \widetilde{\nabla}_{\vec{\Phi}(\tilde{q})} \vec{\Phi}(\tilde{r}) - \widetilde{\nabla}_{\vec{\Phi}(\tilde{q})} \widetilde{\nabla}_{\vec{\Phi}(\tilde{p})} \vec{\Phi}(\tilde{r}) + \widetilde{\nabla}_{[\vec{\Phi}(\tilde{p}), \vec{\Phi}(\tilde{q})]} \vec{\Phi}(\tilde{r}) \right\rangle \\ &= \frac{1}{4} \sum_{\sigma_l, s_l}^{\tilde{l}=\tilde{k}-\tilde{p}} \frac{((- \tilde{k} \| \tilde{p} \| \tilde{l}))}{g(\tilde{k})} \frac{((- \tilde{l} \| \tilde{q} \| \tilde{r}))}{g(\tilde{l})} (\lambda(\tilde{p}) - \lambda(\tilde{l}) - \lambda(\tilde{k})) (\lambda(\tilde{q}) - \lambda(\tilde{r}) - \lambda(\tilde{l})) \\ &\quad - \frac{1}{4} \sum_{\sigma_m, s_m}^{\tilde{m}=\tilde{k}-\tilde{q}} \frac{((- \tilde{k} \| \tilde{q} \| \tilde{m}))}{g(\tilde{k})} \frac{((- \tilde{m} \| \tilde{p} \| \tilde{r}))}{g(\tilde{m})} (\lambda(\tilde{q}) - \lambda(\tilde{m}) - \lambda(\tilde{k})) (\lambda(\tilde{p}) - \lambda(\tilde{r}) - \lambda(\tilde{m})) \\ &\quad + \frac{1}{2} \sum_{\sigma_n, s_n}^{\tilde{n}=\tilde{k}-\tilde{r}} \frac{((- \tilde{k} \| \tilde{n} \| \tilde{r}))}{g(\tilde{k})} \frac{((- \tilde{n} \| \tilde{p} \| \tilde{q}))}{g(\tilde{n})} (\lambda(\tilde{n}) - \lambda(\tilde{r}) - \lambda(\tilde{k})) \lambda(\tilde{n}), \end{aligned} \quad (27)$$

where λ is the eigenvalue of the helicity-based, particle-relabeling operator \widehat{W} (see (52) and (54)), the tilde notation with a minus sign $(-\tilde{k})$ represents $(-\tilde{k}, \sigma_k, s_k)$. Note that the relation $\lambda(-\tilde{k}) = \lambda(\tilde{k})$ holds. The explicit expression of the three-mode parenthesis symbol $((* \| * \| *))$ is given by (66). The details of the expressions, formulae, and equations related to the GEV representation are summarized in Appendix 3. As can be seen from Equation (26), the Riemannian curvature term contains four-wave resonances, while the other terms are decoupled for each GEV mode.

3.3. Statistical homogeneity and isotropy assumption and normal mode representation of sectional curvature

Since our principal interest is the statistical features of turbulent solutions of HMHD systems, we address the ensemble average of reference solutions $\vec{V}(t)$. Assuming that the reference solutions are random vector fields that are statistically homogeneous and isotropic and that main flow and perturbation are independent each other, we introduce here the correlation function $Q(k, \sigma_k, s_k; t)$ that satisfies

$$\left\langle \widehat{V}(\tilde{k}; t) \widehat{V}(\tilde{p}; t) \right\rangle = Q(|\tilde{k}|, \sigma_k, s_k; t) \delta_{\sigma_k \sigma_p} \delta_{s_k s_p} \delta_{-\tilde{k}, \tilde{p}}^3, \quad (28)$$

where the angled brackets without vertical bars $\langle * \rangle$ denote the ensemble average and δ and δ^3 denote the Kronecker delta and its triple product, respectively. This assumption imposes the wavenumber relation $\vec{r} = -\vec{q}$, and $\vec{p} = \vec{k}$ and simplifies the curvature term considerably. Thus, the Jacobi Equation (26) is reduced to

$$\begin{aligned} \frac{1}{2} \frac{\partial}{\partial t} \left(|\widehat{\xi}(\tilde{k}; t)|^2 + |\widehat{\eta}(\tilde{k}; t)|^2 \right) &= \overline{\widehat{\xi}(\tilde{k}; t)} \widehat{\eta}(\tilde{k}; t) \\ &- \sum_{\vec{p}, \sigma_p, s_p} R_H(k, \sigma_k, s_k, p, \sigma_p, s_p, q, \alpha) Q(p, \sigma_p, s_p; t) \widehat{\xi}(\tilde{k}; t) \overline{\widehat{\eta}(\tilde{k}; t)} \end{aligned} \quad (29)$$

for each GEV mode \tilde{k} , where $q := |\vec{k} - \vec{p}|$, and R_H is defined by

$$\begin{aligned} R_H(k, \sigma_k, s_k, p, \sigma_p, s_p, q, \alpha) &:= g(\tilde{k})^{-1} \left\langle \overline{\vec{\Phi}(\tilde{k})} \left| R(\vec{\Phi}(\tilde{k}), \vec{\Phi}(\tilde{p})) \vec{\Phi}(-\tilde{p}) \right\rangle, \\ &= R_1(k, \sigma_k, s_k, p, \sigma_p, s_p, q, \alpha) + R_2(k, \sigma_k, s_k, p, \sigma_p, s_p, f(q), \alpha), \end{aligned} \quad (30)$$

$$R_1(k, \sigma_k, s_k, p, \sigma_p, s_p, m, \alpha) = \sum_{\sigma_m, s_m}^{\vec{m}=\vec{k}-\vec{p}} \frac{\left| \left((-\tilde{k} \parallel \tilde{p} \parallel \tilde{m}) \right) \right|^2}{4 g(\tilde{k}) g(\tilde{m})} \left[\left(\lambda(\tilde{p}) - \lambda(\tilde{k}) \right)^2 - \lambda(\tilde{m})^2 \right], \quad (31)$$

$$R_2(k, \sigma_k, s_k, p, \sigma_p, s_p, n, \alpha) = \sum_{\sigma_n, s_n}^{\vec{n}=\vec{k}+\vec{p}} \frac{\left| \left((-\tilde{n} \parallel \tilde{k} \parallel \tilde{p}) \right) \right|^2}{2 g(\tilde{k}) g(\tilde{n})} \lambda(\tilde{n}) \left(\lambda(\tilde{p}) + \lambda(\tilde{k}) - \lambda(\tilde{n}) \right), \quad (32)$$

$f(q) := |\vec{k} + \vec{p}| = \sqrt{2k^2 + 2p^2 - q^2}$. The reduced curvature tensor R_H is the sectional curvature between two GEV modes \spadesuit . We call R_H the GEV-mode sectional curvature in the following.

Equation (29) can be rewritten as simultaneous equations for each GEV mode as follows:

$$\frac{d}{dt} \begin{pmatrix} \widehat{\xi}(\tilde{k}; t) \\ \widehat{\eta}(\tilde{k}; t) \end{pmatrix} = \begin{pmatrix} 0 & 1 \\ -\sum_{\vec{p}} R_H(\tilde{k}, \tilde{p}, q, \alpha) Q(p, \sigma_p, s_p; t) & 0 \end{pmatrix} \begin{pmatrix} \widehat{\xi}(\tilde{k}; t) \\ \widehat{\eta}(\tilde{k}; t) \end{pmatrix}. \quad (33)$$

Note that the GEV-mode sectional curvatures do not depend directly on their wavenumber vectors, but rather on their moduli (k and p) and the angle between them ($q = k^2 + p^2 - 2kp \cos \theta$). The explicit expression of the the GEV-mode sectional curvature is given by Equation (68) in Appendix 4.

\spadesuit Mathematically, the sectional curvature is defined by $K = \langle \vec{\xi} | R(\vec{\xi}, \vec{V}) \vec{V} \rangle / \left(\langle \vec{\xi} | \vec{\xi} \rangle \langle \vec{V} | \vec{V} \rangle - \langle \vec{\xi} | \vec{V} \rangle^2 \right)$, and does not agree with R_H unless each of $\vec{\xi}$ and \vec{V} is a single GEV-mode.

Assuming isotropy and approximating the summation with respect to \vec{p} by the three-dimensional integral, ($\sum_{\vec{p}} \approx \iiint d^3\vec{p}$), we can obtain the following formula:

$$\begin{aligned} & \sum_{\vec{p}, \sigma_p, s_p} R_H(k, \sigma_k, s_k, p, \sigma_p, s_p, q, \alpha) Q(p, \sigma_p, s_p; t) \\ & \approx \sum_{\sigma_p, s_p} \int_0^\infty dp K_H(k, \sigma_k, s_k, p, \sigma_p, s_p, \alpha) Q(p, \sigma_p, s_p; t), \end{aligned} \quad (34)$$

where the integration kernel function K_H is given by

$$K_H(k, \sigma_k, s_k, p, \sigma_p, s_p, \alpha) = \frac{2\pi p}{k} \int_{|\vec{k}-\vec{p}|}^{k+p} dq \left[q R_H(k, \sigma_k, s_k, p, \sigma_p, s_p, q, \alpha) \right]. \quad (35)$$

Hereafter we call K_H the shell-averaged curvature kernel. The explicit expression of the shell-averaged curvature kernel is given by Equation (69) in Appendix 4. Note that the GEV-mode sectional curvature and the shell-averaged curvature kernel are, by definition (30), symmetric with exchange of k and p .

Since the Fourier transform of the correlation function, $Q(p, \sigma_p, s_p; t)$, is positive definite, the sign of the curvature is determined solely by the sign of the shell-averaged curvature kernel K_H . Moreover, the contribution of the interaction between the perturbation (\vec{k}) and the main flow (\vec{p}) to K_H is measured by the (p, q) -plane distribution of the GEV-mode sectional curvature R_H for assigned \vec{k} .

4. Sectional curvature analysis of hydrodynamic and magnetohydrodynamic stabilities

In this section, we observe the functional features of the sectional curvatures and discuss their implications for the stabilities of the basic flows. Before embarking on a detailed analysis, some remarks should be made.

The normal-mode sectional curvatures for the HMHD and HD systems are decomposed into a product of the square of the wavenumber of the perturbation $\pi^2 k^2$ and a dimensionless function \widehat{R} : $R = \pi^2 k^2 \widehat{R}$. Furthermore, the GEV-mode sectional curvature for the HMHD system (68) is given by a series of functions of the wavenumber moduli ratios $\underline{p} := p/k$ and $\underline{q} := q/k$ as $R_H(k, p, q) = \pi^2 k^2 \sum_n (\pi \alpha k)^n \widehat{R}_H^{(n)}(\underline{p}, \underline{q})$, where the dimensionless expansion parameter $\pi \alpha k$ measures the scale disparity ratio of the ion skin depth to the observed perturbation scale. As for the HD case, the CHW-mode sectional curvature (82) has the following form: $R_E(k, p, q) = \pi^2 k^2 \widehat{R}_E(\underline{p}, \underline{q})$.

This leads to two important consequences: first, the stability features of the systems, i.e., the sign of R s are determined by the dimensionless functions, $\widehat{R}_H^{(n)}$ or \widehat{R}_E . Second, these functions are scale-independent because they are the function of the wavenumber moduli ratios $\underline{p} := p/k$ and $\underline{q} := q/k$. In other words, the stability features do not depend directly on the wavenumber vectors of the main flow \vec{p} and the perturbation \vec{k} , but on their relative scale disparity and angle between them, i.e., the geometrical shape of the triangle formed by $\{\vec{k}, \vec{p}, \vec{k} - \vec{p}\}$ (irrespective of its orientation).

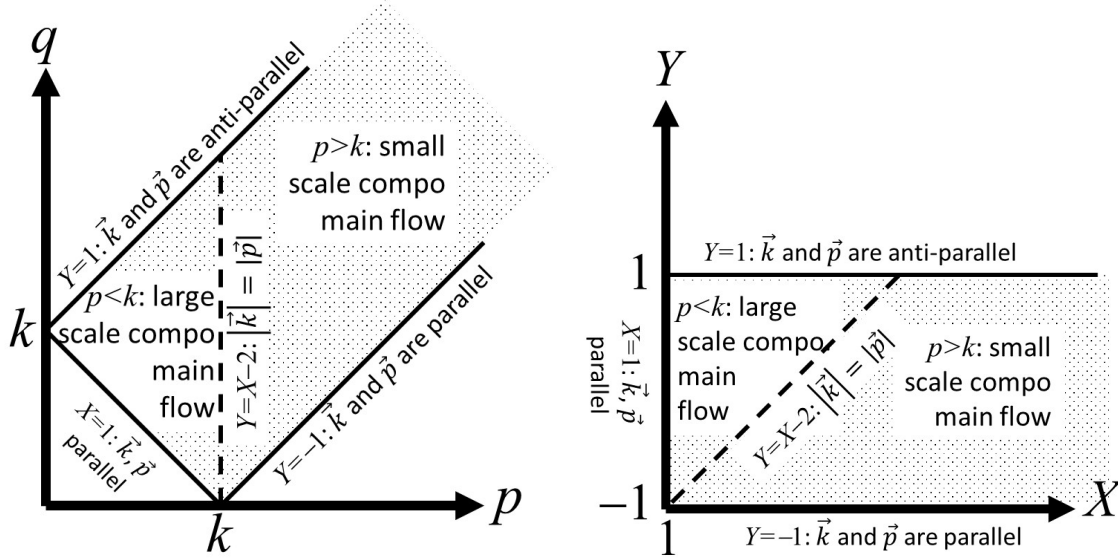


Figure 2. How to read the following figures of geometric factors of normal-mode sectional curvature \hat{R} . Left: Region wherein moduli (k, p, q) of resonant three waves constitute a triangle in (p, q) -space for an assigned k . Right: Region is inclined clockwise by 45 degrees, and the coordinates are normalized by k ; abscissa: $X = \underline{p} + \underline{q} > 1$, ordinate: $-1 < Y = \underline{q} - \underline{p} < 1$. Top left corner region close to $(X, Y) \approx (1, 1)$ corresponds to $0 \approx p \ll k \approx q$, i.e., the influence of large-scale components (or “nonlocal” interaction) of main flow on perturbation. In contrast, region close to line $Y = X - 2$ reads “local” ($k \approx p$) interaction. Region to right of $Y = X - 2$ describes influence of small-scale components of main flow.

Thus, we will present in the following sections the dimensionless functions \hat{R} s, which are called “geometric factors” hereafter, instead of R s. An explanation of how to read the functional profiles of the geometric factors is given in Fig. 2.

In the following we use the term “nonlocal” when the considered spatial scales of main flow and perturbation differ significantly each other. In terms of the disparity ratio of wavenumbers $\underline{p} = p/k$, the term “nonlocal” implies the characteristic features around $\underline{p} \approx 0$ (or $\underline{p} \gg 1$), or the tendencies of some properties for $\underline{p} \rightarrow 0$ (or $\underline{p} \rightarrow +\infty$). The term “local” is used when the features or tendencies are not “nonlocal.” The use of these terms are not so strict.

4.1. Stability of Euler dynamics

For comparison with the HMHD case, we examine the HD case, i.e., the case wherein the magnetic field is absent.

As was discussed in [25], the dissipationless, incompressible HD, MHD, and HMHD systems have common mathematical structures. Thus, the formal derivations of differential-geometrical properties and equations such as given in the previous two

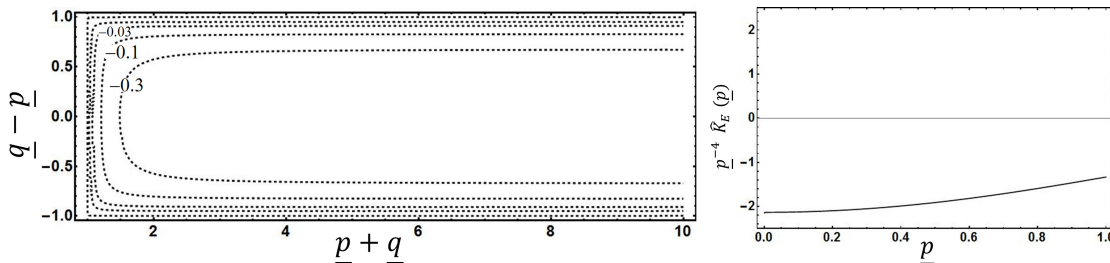


Figure 3. Left: Geometric factor of CHW-mode sectional curvature of Euler dynamics, $\widehat{R}_E(\underline{p}, \underline{q})$, drawn in range $1 < \underline{p} + \underline{q} < 10$, $-1 < \underline{q} - \underline{p} < 1$. Contour levels are set to $-10^{N/2}$ ($N \geq -7$). Right: Geometric factor of shell-averaged curvature kernel (divided by \underline{p}^4), $\underline{p}^{-4} \widehat{K}_E(\underline{p})$, drawn in range $0 < \underline{p} < 1$. All of the values are independent of helicity parameters σ_k and σ_p .

sections are also applicable to the Euler equation case. The explicit expressions of the Riemannian metric, Lie bracket, Levi-Civita connection, and sectional curvature for the representation using the complex helical wave (CHW), which is known as the basis function of three-dimensional solenoidal fields [30], are summarized in Appendix 5.

First of all, the sectional curvature $R_E(k, \sigma_k, p, \sigma_p, q)$ is negative definite for arbitrary two CHWs (see Eq. (82)). In the left panel of Figure 3, we presented the functional form of the geometric factor of the sectional curvature $\widehat{R}_E(\underline{p}, \underline{q})$. This plausibly implies that the Euler dynamics is always unstable for arbitrary perturbation. The negative sectional curvature between two monochromatic waves was already reported by Nakamura et al. [5]. Our novel findings are that this feature is independent of the helicities σ of the main flow and perturbation, and that the $(\underline{p}, \underline{q})$ -plane distribution of sectional curvature amplitude is presented.

As for the application to homogeneous and isotropic turbulet flows, on the other hand, the sectional curvature should be accumulated by the spherical shells in wavenumber space (see Equation (34)). In the right panel of Figure 3, the geometric factor of the shell-averaged curvature kernel for the Euler dynamics (83) is presented.

Note that in the right panel of the Fig. contour Euler the infrared side ($0 < \underline{p} < 1$) of $(\underline{p}, \underline{p}^{-4} \widehat{K}_E(\underline{p}))$ is plotted where the factor \underline{p}^{-4} is multiplied to grasp the $\underline{p} \rightarrow 0$ tendency of \widehat{K}_E . As for the ultraviolet side ($\underline{p} > 1$), it is checked that the plot of $(\underline{p}^{-1}, \underline{p}^2 \widehat{K}_E(\underline{p}^{-1}))$ for $0 < \underline{p}^{-1} < 1$ gives the same functional profile as this graph.

Since the regularity of the curvature kernel is $O(\underline{p}^4)$ for small \underline{p} , the sectional curvature (34) for the correlation function with the scaling $Q(p) \propto p^\gamma$ converges in the infrared side if $\gamma > -5$. For the ultraviolet side, the sectional curvature integral converges for $\gamma < -3$ due to the $O(\underline{p}^{-2})$ tendency for large \underline{p} . It is very interesting that $\gamma = -11/3$, which corresponds to Kolmogorov's 1941 inertial range scaling law, is included in this convergent range. Thus, the sectional curvature of the Euler dynamics is negative definite, and the interaction between the main flow and the perturbation is "local" in the sense that the integration does not diverge on either the infrared side or

the ultraviolet side.

4.2. $O(\alpha^0)$ features of HMHD dynamics: MHD system stability

In Figure 4, the GEV-mode sectional curvature for the MHD case (i.e. the $\alpha \rightarrow 0$ limit case) is presented.

In contrast to the Euler dynamics case, two remarkable features are seen: firstly, the stability of the MHD dynamics depended on the helicity combinations of the main flow and perturbation, as well as depending on their linear-mode-branch combinations.

Furthermore, the mode sectional curvatures take both positive and negative values, i.e., there are both stable and unstable wavenumber combinations. In particular, all of the sectional curvatures are positive around the regions with $\underline{p} \approx \underline{q} \approx 0$ (upper left corner of each panel) and those with $\underline{p}, \underline{q} \gg 1$ (far beyond the right side of each panel), which implies that such the interactions that is “nonlocal” in wavenumber space do not lead to the growth of small perturbations. In other words, this conjectures that the main flow destabilization is essentially caused by the “local” mode interactions in the MHD case.

Let us see some of the details of the sectional curvature profiles.

The upper and middle panels of Fig. 4 depict the stability of waves that belong to the same linear-mode-branch ($s_k = s_p$). Negative values of $\widehat{R}_H^{(0)}$ appear around $k \approx p \gg q$ for $\sigma_k = \pm\sigma_p$ and $k \approx p \approx q/2$ for $\sigma_k = \sigma_p$. These wavenumber modulus relations indicate that the interactions between the waves whose wavenumbers are nearly parallel ($\vec{k} \parallel \vec{p}$) destabilize the main flow.

However, the stable wavenumber combinations are roughly perpendicular, i.e., they satisfy $\vec{k} \perp \vec{p}$ approximately. It is well known that Alfvén waves (with wavenumber \vec{k}) propagate most efficiently in the direction of the ambient magnetic field \mathbf{B} , i.e., $\mathbf{B} \parallel \vec{k}$. Since \mathbf{B} is solenoidal, $\mathbf{B} \perp \vec{p}$, and thus it is expected that the stable region is dominated mainly by the propagation of Alfvén waves.

The middle and lower panels of Fig. 4 give the stability of the waves in the opposite linear-mode-branch ($s_k = -s_p$). It is remarkable that the interactions between the different helicities ($\sigma_k = -\sigma_p$) are unstable irrespective of the angles between the wavenumbers of the main flow and the perturbation.

As for the application to homogeneous and isotropic turbulent flows, on the other hand, the sectional curvature should be accumulated by the spherical shells in wavenumber space (see Equation (34)). The right-hand panels of Fig. 4 show the functional profiles of the geometric factor of the shell-averaged sectional curvature kernel $\widehat{K}_H^{(0)}$ (multiplied by \underline{p}^{-2}) for $0 < \underline{p} < 1$. Note that, the plot of $(\underline{p}^{-1}, \underline{p}^4 \widehat{K}_E(\underline{p}^{-1}))$ for $0 < \underline{p}^{-1} < 1$ gives the same functional profile.

Since $\widehat{R}_H^{(0)}(\underline{p}, \underline{q})$ takes both the positive and negative values for some assigned \underline{ps} , the kernel function $\widehat{K}_H^{(0)}(\underline{p})$ tends to have positive (stable) value even for such wavenumbers \underline{p} that have negative sectional curvature (unstable) combinations $(\underline{p}, \underline{q})$. Due to this

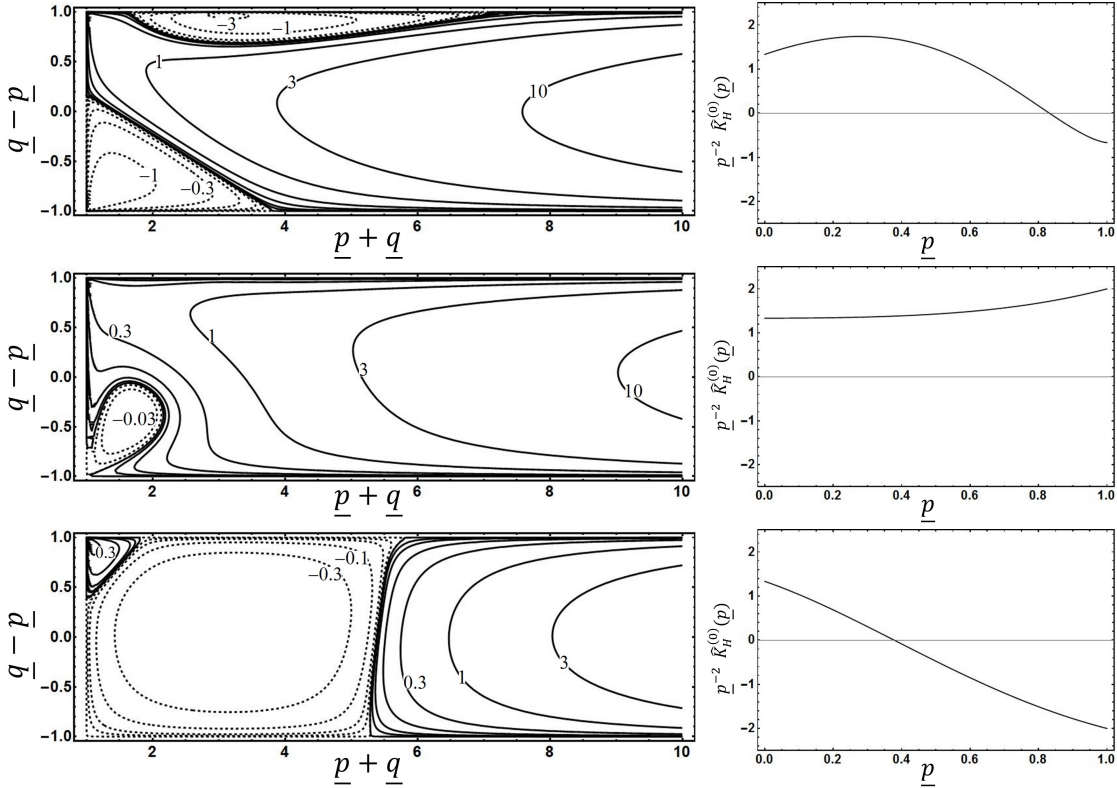


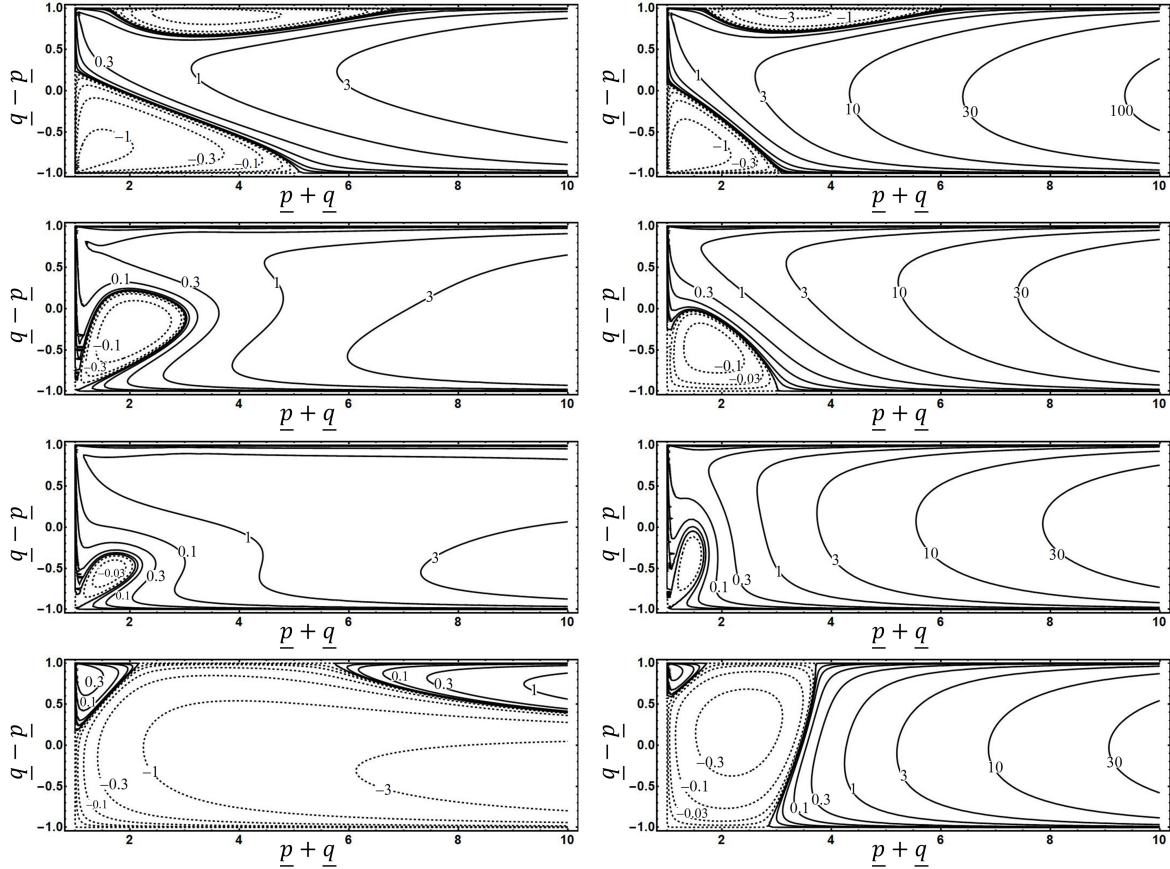
Figure 4. Left: Geometric factor of GEV-mode sectional curvature of the MHD dynamics, $\widehat{R}_H^{(0)}(p, q, \sigma_k \sigma_p, s_k s_p)$. The range shown is same as that in Fig. 3. Solid (dashed) contour lines denote positive (negative) values; their levels are set to $10^{N/2}$ ($-10^{N/2}$) for $N \geq -7$. Right: Corresponding geometric factors of shell-averaged curvature kernel (divided by p^2) $p^{-2} \widehat{K}_H^{(0)}(p, q, \sigma_k \sigma_p, s_k s_p)$ in range $0 < p < 1$. Mode combinations are $s_k s_p = \sigma_k \sigma_p = 1$ (upper), $s_k s_p = -\sigma_k \sigma_p = \pm 1$ (middle), and $s_k s_p = \sigma_k \sigma_p = -1$ (lower).

summation process, the negative values of the kernel function appear only for those cases with $\sigma_k \sigma_p = s_k s_p$. The unstable ranges are $0.8318 < \underline{p} < 1/0.8318$ for $\sigma_k \sigma_p = s_k s_p = 1$ and $0.3784 < \underline{p} < 1/0.3784$ for $\sigma_k \sigma_p = s_k s_p = -1$. This result suggests that the contribution of the mode interactions to the plasma motion stability should be analyzed more carefully than by integrating the sectional curvature simply.

It is interesting that the shell-averaged curvature kernel behaves as $K_H^{(0)}(k, p) \approx \frac{4}{3} \pi^3 k^4 \underline{p}^2 + o(\underline{p}^2)$ irrespective of the values of σ and s for sufficiently small p . The value is analytically obtained by expanding Equation (73) in power series of \underline{p} around $\underline{p} = 0$. As will be discussed in the final section, this conjectures that the interaction with large scale components of plasma motions is dominated by the propagation of Alfvén waves.

4.3. $O(\alpha^1)$ features of the HMHD dynamics: lowest-order Hall-term effect

In this section, we examine the geometric factor including the $O(\alpha)$ terms of the GEV-mode sectional curvature, $\widehat{R}_H^{(0)} + \pi \alpha k \widehat{R}_H^{(1)}$, for the dimensionless parameter $\alpha k = 0.1$.


Figure 5.

Geometric factor including the $O(\alpha)$ terms of GEV-mode sectional curvature, $\widehat{R}_H^{(0)} + 0.1\pi\widehat{R}_H^{(1)}$. Helicity and linear-mode-branch parameters are summarized in table on the right. Range and contour levels plotted are same as those in Fig. 4.

| row | $\sigma_k\sigma_p$ | left | | right | |
|-----|--------------------|-------|-------|-------|-------|
| | | s_k | s_p | s_k | s_p |
| 1 | 1 | 1 | 1 | -1 | -1 |
| 2 | -1 | 1 | 1 | -1 | -1 |
| 3 | 1 | -1 | 1 | 1 | -1 |
| 4 | -1 | -1 | 1 | 1 | -1 |

The detailed expression of $\widehat{R}_H^{(1)}$ is given by Eq. (75). We focus here how the Hall-term effect at the lowest order changes the stability diagram of the MHD system (see Fig. 4). In Figure 5, the $(\underline{p}, \underline{q})$ -space distributions for all possible combinations of σ_k , σ_p , s_k , and s_p are presented.

The panels are arranged according to the displaying order of Fig. 4 in the vertical direction. The left (right) four panels show the contribution of ion cyclotron (whistler) modes to the stability. As is seen from the figure, the contribution of the ion cyclotron mode ($s_p = 1$) by the Hall-term effect is somewhat opposite to that of the whistler mode ($s_p = -1$).

In the three of four cases (except for $(s_k, s_p) = (-1, 1)$), the ion cyclotron mode of the reference flow enhances the unstable mode combination regions. Especially, for the combination with whistler mode with opposite helicity (the 4-th row of Fig. 5), the unstable region is significantly spread over and the amplitude of the negative sectional

curvature is enhanced (compared with other seven panels). This tendency physically implies that, due to the Hall-term effect, the ion cyclotron modes tend to excite the whistler modes more efficiently than other mode combinations.

On the other hand, in the three of four cases of (except for $(s_k, s_p) = (-1, -1)$), the Hall-term effect suppresses the instability due to the whistler mode of the reference solution, i.e., reduces the unstable mode combination regions. The amplitudes of the positive (stable) sectional curvature region, i.e., the characteristic time or frequency of the perturbation fields significantly increased compared with the MHD and the ion cyclotron mode of HMHD cases. It is guessed that, since the whistler modes have large phase velocities, they disperse more quickly than the unstable modes grow.

As a whole, the result conjectures an interesting picture that the ion cyclotron modes excite the whistler mode, while the excited whistler modes disperse quickly. Thus the energy is transferred from the ion cyclotron modes to the whistler ones in an almost one-sided way. This picture is partly supported by the direct numerical simulation result of the fully-developed HMHD turbulence [31].

5. Summary and discussion

In the present study, we approached the linear stability problem of the HMHD system using geodesic formulation and considered its applicability to turbulence theory.

Geodesic formulation, normal-mode expansion, and application to turbulence: The evolution equation of a dissipationless, incompressible HMHD fluid was formulated as a geodesic equation from a direct product of two volume-preserving diffeomorphisms. Instead of usual mathematical postulation, we considered the linear connection ($\tilde{\nabla}$) from the viewpoint of physically desirable properties that 1) reproduced the Euler–Lagrange equation as its geodesic, 2) guaranteed the detailed energy balance, and 3) made the associated substantial derivative $\partial_t + \tilde{\nabla}_{\vec{v}}$ covariant against the Galilean boost. The obtained connection agreed with the Levi-Civita connection. It was an interesting finding that the Levi-Civita connection had these physically desirable properties for the HMHD (finite α), MHD ($\alpha \rightarrow 0$), and HD ($\alpha = 0$) cases.

We performed stability analysis in terms of the Jacobi equation. Lin constraints ($\frac{D}{Dt}\vec{\xi} - \tilde{\nabla}_{\vec{\xi}}\vec{V} = \vec{v}$) and the linearized equation of motion ($\frac{D}{Dt}\vec{v} + \tilde{\nabla}_{\vec{v}}\vec{V} = 0$) gave the Jacobi equation ($(\frac{D}{Dt})^2\vec{\xi} + R(\vec{\xi}, \vec{V})\vec{V} = 0$). It was also discussed that the analysis method based on the Jacobi equation is applicable to the problems of both the linear stability of basic flow and the relative dispersion of passively advected particle pairs. The sign of the Riemannian curvature tensor $R(*, \vec{V})\vec{V}$ was used to determine the stability of the reference solution \vec{V} .

Normal-mode stability analysis was carried out by using the GEV-mode expansion. The difficulty that the Riemannian curvature term contains four-wave resonance was reduced by taking ensemble average of random vector fields (fully-developed turbulence). Since the reduced curvature term naturally includes the sectional curvature between two

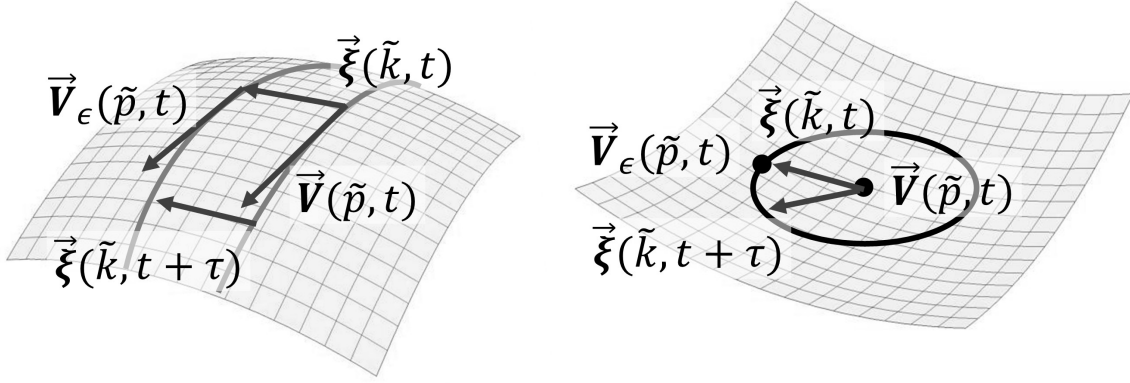


Figure 6. In the Lagrangian mechanics, a stationary solution is expressed by a path $e^{t\vec{V}}$ on a *configuration* space. In the Hamiltonian mechanics, on the other hand, a stationary solution is expressed by a fixed point on a *phase* space. In both cases, the stability condition is evaluated by the growth of some appropriate norm of perturbation fields $\|\vec{\xi}(t)\|$. If the perturbation norm is proved to be bounded, the solution satisfy the sufficient condition for the stability.

GEV-mode, the curvature analysis was also able to be interpreted as the stability of a single GEV-mode.

Remark on applicability of normal-mode expansion other than GEVs: the normal-mode expansion expression of the Levi–Civita connection Eq. (67) and the Riemannian curvature tensor Eq. (27) had its foundation on the formula that the combination of the Riemannian metric and the Lie bracket is equal to the product of the eigenvalue of the helicity-based, particle-relabeling operator and a certain totally antisymmetric tensor, $\langle \vec{\Phi}(\tilde{k}) | [\vec{\Phi}(\tilde{p}), \vec{\Phi}(\tilde{q})] \rangle = \lambda(\tilde{k}) (\tilde{k} \| \tilde{p} \| \tilde{q})$. As was described in Ref. [25], this decomposition formula is based on the general eigenvalue problem that derives the DBFs under appropriate boundary condition. Thus, the expression of the curvature tensor is applicable to the systems with arbitrary shape, for example, to cylindrical configuration.

Comparison with other stability analyses: The stability of the HMHD system had often been analysed in the Hamiltonian mechanical framework. One of the well-known method is the energy-Casimir method, in which the second variation of an appropriate functional, i.e., the Hamiltonian with some other constants of motion is calculated as a sufficient condition for the stability of stationary solution (e.g. [3]; §1.7).

As for the HMHD system, the Hamiltonian formulation was developed by Holm and the stability conditions were investigated [17]. An important improvement of the variational procedure was made by Hirota et al., in which the kind of variations were categorized in a sophisticated manner [19]. They distinguished among the following three kinds of perturbation fields: arbitrary perturbation, Lagrangian displacements, and dynamically accessible variation.

From the viewpoint of physical objects and their implications, our method seems almost equivalent to their “Lagrangian displacements” variation, because the followings have their counterparts: choice of the variation fields that satisfy Lin constraints (21) (Eqs. (12) and (13) of [19]), derivation of their evolution equation (22) (Eqs. (26) and (30) of [19]), and calculation of the norm of the variation fields (25) (Eqs. (35)-(38) of [19]). Thus, the GEV-mode sectional curvature analysis is also interpreted as a concrete evaluation of the “Lagrangian displacement” type of the Hamiltonian stability condition for the stationary solutions given by the GEVs, though the pictures of the Lagrangian and Hamiltonian mechanics are qualitatively different each other (see Fig. 6).

It should be remarked that the most important advantage of the sectional curvature analysis is that, compared with the Hamiltonian mechanical variational method, it is applicable to the stability analysis of non-stationary solutions including turbulence.

Results of normal-mode analysis and implication for turbulence: We examined the HD ($\alpha = 0$) and MHD ($\alpha \rightarrow 0$) systems and the $O(\alpha)$ contribution of the Hall-term effect.

The most important and unexpected finding was that the sectional curvature analysis of the MHD system between two GEV modes derives both the stable (positive curvature) and unstable (negative curvature) mode interactions. This characteristic was in sharp contrast to the behavior of the HD system in which the value of the sectional curvature between two arbitrary CHW modes was negative, i.e., the hydrodynamic flow was always unstable.

Furthermore, the GEV-mode solution was always stable if the combination of the wavenumbers of the reference solution (\vec{p}) and perturbation (\vec{k}) was nonlocal ($|\vec{k}|/|\vec{p}| \approx 0$ or $|\vec{k}|/|\vec{p}| \gg 1$), i.e., their characteristic spatial scales differ significantly. Conversely, the instability occurred only when their spatial scales were relatively close, i.e., the interaction was local.

One possible explanation for the positive sectional curvatures in the MHD case is the propagation of waves. For example, the positive curvatures at small p can be explained by the Alfvén waves (see Appendix 6). It is expected that the qualitative physical feature is retained when the wavenumbers gradually change without change the sign of the sectional curvature.

As for the negative curvature, besides wavy plasma motion, the evolution equation (1) can be rewritten as

$$\partial_t(\alpha\boldsymbol{\omega} + \mathbf{b}) = \nabla \times [\mathbf{v} \times (\alpha\boldsymbol{\omega} + \mathbf{b})], \quad \partial_t \mathbf{b} = \nabla \times [(\mathbf{v} - \alpha\mathbf{j}) \times \mathbf{b}], \quad (36)$$

which implies that the field lines of $\alpha\boldsymbol{\omega} + \mathbf{b}$ (\mathbf{b}) are frozen-in, i.e., advected by \mathbf{v} ($\mathbf{v} - \alpha\mathbf{j}$). As discussed in [25], the “generalized vorticity” of the Euler, HMHD, and MHD equations have a common mathematical structure that implies the generalized vorticity fields are frozen-in. Thus, it is expected that the stretching of field lines occurs according to the motion of the ion and electron fluids, which seems to cause dynamo action or turbulent plasma motion.

A conceptual picture is required to understand consistently the coexistence of

such non-growing (possibly wavy) and unstable, growing (possibly chaotic or turbulent) motions, but the development of such a picture is left as future work.

As for the application to turbulence, taking ensemble average and assuming homogeneity and isotropy, we reduced the problem to one of the sectional curvature analysis: $\langle R(*, \vec{V})\vec{V} \rangle(\vec{k}) = \pi^3 k^4 \int d\underline{p} \widehat{K}(\underline{p}) Q(k\underline{p})$, where $\underline{p} := p/k$, \widehat{K} is the shell-averaged curvature kernel, and $Q = \langle \widehat{V}\widehat{V} \rangle$ is the correlation function of the generalized velocity. Thus, the stability properties does not depend only on the normal-mode sectional curvature, but also on the spectrum of the correlation function.

Sectional curvature analysis conjectures that the *local* mode interactions are relevant to the instability for both the HD and MHD cases. That is, the interactions of such modes with close characteristic spatial scales evoke the flow instability. However, the reasons are quite different from each other. For the HD case, since the sectional curvature is small enough around $p \approx 0$, the integral $\int d\underline{p} \widehat{K}(\underline{p}) Q(k\underline{p})$ converges when $Q(p) \propto p^\gamma$ for $\gamma > -5$ in the infrared side, which includes the famous Kolmogorov 1941 spectrum $Q(p) \propto p^{-11/3}$. That is, although nonlocal interactions are intrinsically destabilizing, their influence is small enough. For the MHD case, on the other hand, the sectional curvature itself is negative only for the local interactions.

Acknowledgments

The author is grateful to Prof. S. Yanase for useful comments and to Prof. H. Miura for his continuous encouragement. The author also expresses sincere thanks to the anonymous referees for their helpful comments and suggestions for revising manuscript. This work was performed under the auspices of the NIFS Collaboration Research Program (NIFS13KNSS044, NIFS15KNSS065) and KAKENHI (Grant-in-Aid for Scientific Research(C)) 23540583. The author would like to thank Enago for the English language review.

Appendix 1. Galilean invariance of substantial derivative

Here we consider the Galilean boost wherein the time and space coordinates are transformed as

$$t' = t, \quad x'^i = x^i - tU^i, \quad (37)$$

where $\mathbf{U} = (U^i)$ is an assigned constant velocity. In this appendix, prime symbols denote the quantities in the frame K' , which moves relative to the reference frame K . Since Galilean boost does not change the distance between or the direction of two arbitrary points at the same instant, arbitrary frozen-in vector fields (e.g., particle displacement fields, say $\boldsymbol{\xi} = \xi^i \frac{\partial}{\partial x^i}$) are invariant under this transformation:

$$\xi^i(\vec{x}, t) \left(\frac{\partial}{\partial x^i} \right)_{\vec{x}} \longrightarrow \xi'^i(\vec{x}', t') \left(\frac{\partial}{\partial x'^i} \right)_{\vec{x}'}, \quad (38)$$

where each component satisfies

$$\xi^i(\vec{x}, t) = \xi'^i(\vec{x}', t') = \xi'^i(\vec{x} - t\mathbf{U}, t). \quad (39)$$

This equation leads to the following relation between the values of the partial derivatives of the components in K and K' :

$$\left(\frac{\partial \xi^i}{\partial t}\right)_{(\vec{x}, t)} = \left(\frac{\partial \xi'^i}{\partial t'}\right)_{(\vec{x}', t')} - U^j \left(\frac{\partial \xi'^i}{\partial x'^j}\right)_{(\vec{x}', t')} \quad (40)$$

$$\left(\frac{\partial \xi^i}{\partial x^k}\right)_{(\vec{x}, t)} = \left(\frac{\partial \xi'^i}{\partial x'^k}\right)_{(\vec{x}', t')}. \quad (41)$$

Since each component of the position of a fluid particle obeys $X'^i(\vec{a}, t') = X^i(\vec{a}, t) - tU^i$, the components of the Eulerian velocity field satisfy

$$V'^i(\vec{X}'(\vec{a}, t'), t') + U^i = V^i(\vec{X}(\vec{a}, t), t). \quad (42)$$

Thus, the time and covariant derivative of frozen-in field $\boldsymbol{\xi}$ that is advected by the fluid flow \mathbf{V} transforms as

$$\partial_t \boldsymbol{\xi} \longrightarrow \partial_{t'} \boldsymbol{\xi}' - (\mathbf{U} \cdot \nabla') \boldsymbol{\xi}', \quad (43)$$

$$\tilde{\nabla}_{\mathbf{V}} \boldsymbol{\xi} \longrightarrow \tilde{\nabla}'_{\mathbf{V}' + \mathbf{U}} \boldsymbol{\xi}'. \quad (44)$$

The invariance of the frozen-in vector field (38) gives rise to the following transformation of the substantial derivative:

$$\partial_t \boldsymbol{\xi} + \tilde{\nabla}_{\mathbf{V}} \boldsymbol{\xi} \longrightarrow \partial_{t'} \boldsymbol{\xi}' + \tilde{\nabla}'_{\mathbf{V}'} \boldsymbol{\xi}'. \quad (45)$$

Thus, the covariance of the substantial derivative requires

$$\tilde{\nabla}'_{\mathbf{U}} \boldsymbol{\xi}' = (\mathbf{U} \cdot \nabla') \boldsymbol{\xi}'. \quad (46)$$

For the HMHD case, considering the Galilean boost of each of the ion and electron fluid motions, the following conditions are required:

$$(\tilde{\nabla}'_{\vec{U}} \vec{\boldsymbol{\xi}}')_i = (\mathbf{U} \cdot \nabla') \boldsymbol{\xi}'_i, \quad (\tilde{\nabla}'_{\vec{U}} \vec{\boldsymbol{\xi}}')_e = (\mathbf{U} \cdot \nabla') \boldsymbol{\xi}'_e, \quad (47)$$

where $\vec{\mathbf{U}} = (\mathbf{U}, \mathbf{U})$, $\vec{\boldsymbol{\xi}}' = (\boldsymbol{\xi}'_i, \boldsymbol{\xi}'_e)$, and $\boldsymbol{\xi}'_i$, $\boldsymbol{\xi}'_e$ are frozen-in vector fields advected by the motions of the ion and electron plasmas, respectively. The ion component of the covariant derivative by \mathbf{U} is given by

$$\begin{aligned} & \left(\tilde{\nabla}'_{\vec{U}} \vec{\boldsymbol{\xi}}'\right)_i = C_1[\boldsymbol{\xi}'_i, \mathbf{U}] + C_2 \left(\vec{L}_{\vec{\boldsymbol{\xi}}'}^\dagger \vec{\mathbf{U}}\right)_i - C_3 \left(\vec{L}_{\vec{U}}^\dagger \vec{\boldsymbol{\xi}}'\right)_i, \\ & = C_1 \nabla' \times (\mathbf{U} \times \boldsymbol{\xi}'_i) + C_2 ((\nabla' \times \mathbf{U}) \times \boldsymbol{\xi}'_i)_S - C_3 ((\nabla' \times \boldsymbol{\xi}'_i) \times \mathbf{U})_S, \\ & = -(C_1 + C_3)(\mathbf{U} \cdot \nabla') \boldsymbol{\xi}'_i. \end{aligned} \quad (48)$$

However, by using Equations (3) and (11), we can obtain the following difference between the ion and electron components of the covariant derivative:

$$\begin{aligned} & \left(\tilde{\nabla}'_{\vec{U}} \vec{\boldsymbol{\xi}}'\right)_i - \left(\tilde{\nabla}'_{\vec{U}} \vec{\boldsymbol{\xi}}'\right)_e \\ & = C_1 ([\boldsymbol{\xi}'_i, \mathbf{U}] - [\boldsymbol{\xi}'_e, \mathbf{U}]) + C_2 \left[\left(\vec{L}_{\vec{\boldsymbol{\xi}}'}^\dagger \vec{\mathbf{U}}\right)_i - \left(\vec{L}_{\vec{\boldsymbol{\xi}}'}^\dagger \vec{\mathbf{U}}\right)_e \right] - C_3 \left[\left(\vec{L}_{\vec{U}}^\dagger \vec{\boldsymbol{\xi}}'\right)_i - \left(\vec{L}_{\vec{U}}^\dagger \vec{\boldsymbol{\xi}}'\right)_e \right], \\ & = C_1 \left[\nabla' \times (\mathbf{U} \times \boldsymbol{\xi}'_i) - \nabla' \times (\mathbf{U} \times \boldsymbol{\xi}'_e) \right] - C_3 \left[\alpha^{-1} (\alpha \nabla' \times)^2 (\mathbf{b}'_\xi \times \mathbf{U}) \right], \end{aligned}$$

$$\begin{aligned}
&= C_1 \left[-(\mathbf{U} \cdot \nabla') \boldsymbol{\xi}'_i + (\mathbf{U} \cdot \nabla') \boldsymbol{\xi}'_e \right] - C_3 \alpha \nabla' \times ((\mathbf{U} \cdot \nabla') \mathbf{b}'_\xi), \\
&= -(C_1 + C_3) (\mathbf{U} \cdot \nabla') (\boldsymbol{\xi}'_i - \boldsymbol{\xi}'_e), \tag{49}
\end{aligned}$$

where $\mathbf{b}'_\xi := \alpha^{-1} (\nabla \times)^{-1} (\boldsymbol{\xi}'_i - \boldsymbol{\xi}'_e)$. Thus, the Galilean boost covariance of the substantial derivative consistently yields the condition $C_1 + C_3 = -1$.

Appendix 2. Remark on applicable stability problems:

The evolution Equation (24) can treat a wider class of problems than those considered by Arnold, despite the comment that he made in his textbook:

“It should be emphasized that instability of a flow of an ideal fluid is here understood differently than in section *K*: it is a question of exponential instability of the *motion of the fluid*, not of its velocity field.” ([4]; app. 2, §L.)

Since the linear stability problem (24) requires two $\vec{\mathbf{V}}$ -variables as initial conditions, we can treat the following two kinds of problems as special cases to the extent that the existence and uniqueness of solutions of Equations (19) and (20) are guaranteed.

- (i) By setting ${}^t(\vec{\boldsymbol{\xi}}(0) \vec{\boldsymbol{\eta}}(0)) = {}^t(\vec{\mathbf{0}} \vec{\mathbf{v}}_0)$, which implies that the fluid particle configurations of the ion and electron fluids are not changed and the $\vec{\mathbf{V}}$ -variable perturbation $\vec{\mathbf{v}}(0) = \vec{\mathbf{v}}_0$ is initially imposed on the reference solution, we can treat the linear stability problem of the *ion and electron fluid velocities*.
- (ii) By setting ${}^t(\vec{\boldsymbol{\xi}}(0) \vec{\boldsymbol{\eta}}(0)) = {}^t(\vec{\boldsymbol{\xi}}_0 \vec{\nabla}_{\vec{\boldsymbol{\xi}}_0} \vec{\mathbf{V}}_0)$, we can obtain a perturbation that satisfies $\vec{\mathbf{v}}(0) = \vec{\mathbf{0}}$, i.e., the initial ion and electron velocities are unchanged. The perturbation field $\vec{\boldsymbol{\xi}}_0$ changes the “labels” of the fluid particle and current field lines so that we can treat the *relative dispersion of particle pairs*, i.e., instability of the *motion of the ion and electron fluids*.

Note that, since we did not specify a particular material for the HMHD system in the above discussion, the latter is applicable in general to geodesically formulated hydrodynamic systems.

Appendix 3. Generalized Elsässer variable representation of differential geometrical quantities

The GEVs were originally derived by Galtier [21] as linear wave modes under the existence of a uniform background magnetic field, \mathbf{B}_0 . In particular, when we consider the standard MHD limit, the GEVs helps us to avoid the singularity problems associated with small values of α [14]. By setting $\alpha \rightarrow 0$, we could obtain the mathematical expressions for the MHD system from the HMHD ones.

The linearized equations for \mathbf{u} and \mathbf{b} are

$$\partial_t (\nabla \times \mathbf{u}) = \nabla \times [(\nabla \times \mathbf{b}) \times \mathbf{B}_0], \quad \partial_t \mathbf{b} = \nabla \times [(\mathbf{u} - \alpha \nabla \times \mathbf{b}) \times \mathbf{B}_0]. \tag{50}$$

Using a \vec{V} -variable, we can rewrite these equations as

$$\frac{\partial}{\partial t} \widehat{W} \begin{pmatrix} \mathbf{V}_i \\ \mathbf{V}_e \end{pmatrix} = \mathbf{B}_0 \cdot \nabla \begin{pmatrix} \mathbf{V}_i \\ \mathbf{V}_e \end{pmatrix}, \quad (51)$$

where the operator \widehat{W} is given by

$$\widehat{W} = \begin{pmatrix} \alpha \nabla \times + (\alpha \nabla \times)^{-1} & -(\alpha \nabla \times)^{-1} \\ (\alpha \nabla \times)^{-1} & -(\alpha \nabla \times)^{-1} \end{pmatrix}. \quad (52)$$

Note that this operator is the helicity-based, particle-relabeling operator with a specific parameter value [14]. Since it contains the curl operator and its inverse, the operator is convenient for decomposing vector fields into complex helical waves (CHWs), each of which is the eigenfunction of the curl operator on \mathbb{T}^3 or E^3 and is given by

$$\phi(\vec{k}, \sigma_k; \vec{x}) := 2^{-\frac{1}{2}} \left(\mathbf{e}_\theta(\vec{k}) + i \sigma_k \mathbf{e}_\phi(\vec{k}) \right) e^{2\pi i \vec{k} \cdot \vec{x}}, \quad (53)$$

where \vec{k} , $\sigma_k = \pm 1$, \mathbf{e}_θ and \mathbf{e}_ϕ are the wavenumber, helicity, and base vectors of the spherical coordinate system on a wavenumber space in the θ - and ϕ -directions, respectively [30]. Using CHWs, we can orthogonally decompose (52) according to \vec{k} and σ_k and obtain the eigenvalue ⁺

$$\lambda(\vec{k}, \sigma_k, s_k, \alpha) = \sigma_k s_k \left(\sqrt{(\pi \alpha |\vec{k}|)^2 + 1} + s_k \pi \alpha |\vec{k}| \right). \quad (54)$$

The eigenfunction corresponding to $\lambda(\vec{k}, \sigma_k, s_k, \alpha)$ is given by ^{*}

$$\vec{\Phi}(\vec{k}, \sigma_k, s_k, \alpha; \vec{x}) = \begin{pmatrix} \lambda(\vec{k}, \sigma_k, s_k, \alpha) \phi(\vec{k}, \sigma_k; \vec{x}) \\ -\lambda(\vec{k}, \sigma_k, -s_k, \alpha) \phi(\vec{k}, \sigma_k; \vec{x}) \end{pmatrix}. \quad (55)$$

Equations (51) and (54), show that the phase velocity of the (\vec{k}, σ_k, s_k) mode is proportional to the product $(\mathbf{B}_0 \cdot \vec{k}) / \lambda(\vec{k}, \sigma_k, s_k, \alpha)$. Thus, the parameter s_k determines the modulus of the phase velocity for each (\vec{k}, σ_k) . The *low-frequency* modes $\vec{\Phi}(\vec{k}, \sigma_k, +, \alpha)$ correspond to the *ion cyclotron waves*, while the *high-frequency* modes $\vec{\Phi}(\vec{k}, \sigma_k, -, \alpha)$ correspond to the *whistler waves*. Despite the fact that the phase velocity of linear waves tends to zero in the limit of vanishing \mathbf{B}_0 or collapses to $\pm \mathbf{B}_0 \cdot \vec{k}$ in the $\alpha \rightarrow 0$ limit, we call $\vec{\Phi}(\vec{k}, \sigma_k, +, \alpha)$ and $\vec{\Phi}(\vec{k}, \sigma_k, -, \alpha)$ the ion cyclotron and whistler modes, respectively, for convenience.

Substituting the GEVs, we can obtain the values of the components of the Riemannian metric tensor (2) as follows:

$$\left\langle \overline{\vec{\Phi}(\vec{k}, \sigma_k, s_k, \alpha)} \left| \vec{\Phi}(\vec{p}, \sigma_p, s_p, \alpha) \right. \right\rangle = (1 + \lambda(\vec{p}, \sigma_p, s_p, \alpha)^2) \delta_{\sigma_k, \sigma_p} \delta_{s_k, s_p} \delta_{\vec{k}, \vec{p}}^3. \quad (56)$$

⁺ The definition of the eigenvalue differs from that in [13] by the sign of s_k . Nevertheless, the correspondence of $s_k = +1$ and -1 to the ion cyclotron and whistler modes, respectively, is unchanged.

^{*} The definition of the eigenfunction is $\lambda(\vec{k}, \sigma_k, s_k, \alpha)$ times larger than that in [13]. Thus, the relationship between the expansion coefficients in the present work and those in [13] is given by $\lambda(\vec{k}, \sigma_k, s_k, \alpha) \widehat{V}(\vec{k}, \sigma_k, s_k; t) = \widehat{Z}(\vec{k}, \sigma_k, s_k; t)$.

When the \vec{V} -variable is expanded in the GEV modes as

$$\vec{V}(\vec{x}, t) = \sum_{\vec{k}, \sigma_k, s_k} \widehat{V}(\vec{k}, \sigma_k, s_k; t) \vec{\Phi}(\vec{k}, \sigma_k, s_k, \alpha; \vec{x}), \quad (57)$$

using the relation (4), we obtain the GEV-coefficient expansion of the ion velocity field \mathbf{u} , current density field \mathbf{j} , and magnetic field \mathbf{b} as

$$\mathbf{u}(\vec{x}, t) = \sum_{\vec{k}, \sigma_k, s_k} \lambda(\vec{k}, \sigma_k, s_k, \alpha) \widehat{V}(\vec{k}, \sigma_k, s_k; t) \boldsymbol{\phi}(\vec{k}, \sigma_k; \vec{x}), \quad (58)$$

$$\mathbf{j}(\vec{x}, t) = 2\pi \sum_{\vec{k}, \sigma_k, s_k} \sigma_k |\vec{k}| \widehat{V}(\vec{k}, \sigma_k, s_k; t) \boldsymbol{\phi}(\vec{k}, \sigma_k; \vec{x}), \quad (59)$$

$$\mathbf{b}(\vec{x}, t) = \sum_{\vec{k}, \sigma_k, s_k} \widehat{V}(\vec{k}, \sigma_k, s_k; t) \boldsymbol{\phi}(\vec{k}, \sigma_k; \vec{x}), \quad (60)$$

where each of the expansion coefficients $\widehat{V}(\vec{k}, \sigma_k, s_k; t)$ is given by

$$\widehat{V}(\vec{k}, \sigma_k, s_k; t) := (1 + \lambda(\vec{k}, \sigma_k, s_k, \alpha)^2)^{-1} \left\langle \overline{\vec{\Phi}(\vec{k}, \sigma_k, s_k, \alpha)} \middle| \vec{V}(t) \right\rangle. \quad (61)$$

Substituting these expressions and using the eigenvalue relations

$$\lambda(\vec{k}, \sigma_k, s_k, \alpha) + \lambda(\vec{k}, \sigma_k, -s_k, \alpha) = 2\pi\alpha\sigma_k|\vec{k}|, \quad (62)$$

$$\lambda(\vec{k}, \sigma_k, s_k, \alpha)\lambda(\vec{k}, \sigma_k, -s_k, \alpha) = -1, \quad (63)$$

we obtain the explicit expression of the combination of the Riemannian metric and the Lie bracket (5) as follows:

$$\begin{aligned} & \left\langle \vec{\Phi}(\vec{k}, \sigma_k, s_k, \alpha) \middle| \left[\vec{\Phi}(\vec{p}, \sigma_p, s_p, \alpha), \vec{\Phi}(\vec{q}, \sigma_q, s_q, \alpha) \right] \right\rangle \\ &= \int_{\vec{x} \in M} d^3\vec{x} \left[(\nabla \times \mathbf{u}_{\vec{k}}) \cdot (\mathbf{u}_{\vec{p}} \times \mathbf{u}_{\vec{q}}) + \mathbf{b}_{\vec{k}} \cdot (\mathbf{u}_{\vec{p}} \times \mathbf{j}_{\vec{q}} + \mathbf{j}_{\vec{p}} \times \mathbf{u}_{\vec{q}} - \alpha \mathbf{j}_{\vec{p}} \times \mathbf{j}_{\vec{q}}) \right]_{\vec{x}} \\ &= \left[\frac{\lambda(\vec{k}) + \lambda(\vec{k}_-)}{\alpha} \lambda(\vec{k}) \lambda(\vec{p}) \lambda(\vec{q}) + \left(\lambda(\vec{p}) \frac{\lambda(\vec{q}) + \lambda(\vec{q}_-)}{\alpha} + \lambda(\vec{q}) \frac{\lambda(\vec{p}) + \lambda(\vec{p}_-)}{\alpha} \right. \right. \\ & \quad \left. \left. - \alpha \frac{\lambda(\vec{p}) + \lambda(\vec{p}_-)}{\alpha} \frac{\lambda(\vec{q}) + \lambda(\vec{q}_-)}{\alpha} \right) \right] \int_{\vec{x} \in M} \boldsymbol{\phi}(\vec{k}, \sigma_k; \vec{x}) \cdot \left(\boldsymbol{\phi}(\vec{p}, \sigma_p; \vec{x}) \times \boldsymbol{\phi}(\vec{q}, \sigma_q; \vec{x}) \right) d^3\vec{x} \\ &= \alpha^{-1} \lambda(\vec{k}) \left(\lambda(\vec{k}) \lambda(\vec{p}) \lambda(\vec{q}) + \lambda(\vec{k}_-) \lambda(\vec{p}_-) \lambda(\vec{q}_-) \right) (\vec{k}, \sigma_k | \vec{p}, \sigma_p | \vec{q}, \sigma_q) \\ &= \lambda(\vec{k}, \sigma_k, s_k, \alpha) ((\vec{k}, \sigma_k, s_k | \vec{p}, \sigma_p, s_p | \vec{q}, \sigma_q, s_q)), \end{aligned} \quad (64)$$

where the notations $\lambda(\vec{k})$ and $\lambda(\vec{k}_-)$ stand for $\lambda(\vec{k}, \sigma_k, s_k, \alpha)$ and $\lambda(\vec{k}, \sigma_k, -s_k, \alpha)$, and the three-mode parenthesis symbols $(\vec{k}, \sigma_k | \vec{p}, \sigma_p | \vec{q}, \sigma_q)$, $((\vec{k}, \sigma_k, s_k | \vec{p}, \sigma_p, s_p | \vec{q}, \sigma_q, s_q))$ are defined by

$$\begin{aligned} (\vec{k}, \sigma_k | \vec{p}, \sigma_p | \vec{q}, \sigma_q) &:= \int_{\vec{x} \in M} \boldsymbol{\phi}(\vec{k}, \sigma_k; \vec{x}) \cdot \left(\boldsymbol{\phi}(\vec{p}, \sigma_p; \vec{x}) \times \boldsymbol{\phi}(\vec{q}, \sigma_q; \vec{x}) \right) d^3\vec{x} \\ &= \frac{e^{i\Psi\{\vec{k}, \vec{p}, \vec{q}\}} |\vec{p} \times \vec{q}|}{2\sqrt{2} |\vec{k}| |\vec{p}| |\vec{q}|} (\sigma_k |\vec{k}| + \sigma_p |\vec{p}| + \sigma_q |\vec{q}|) \delta_{\vec{k} + \vec{p} + \vec{q}, \vec{0}}^3, \end{aligned} \quad (65)$$

$$((\vec{k}, \sigma_k, s_k | \vec{p}, \sigma_p, s_p | \vec{q}, \sigma_q, s_q)) := \alpha^{-1} (\vec{k}, \sigma_k | \vec{p}, \sigma_p | \vec{q}, \sigma_q)$$

$$\begin{aligned} & \times \left(\lambda(\vec{k}, \sigma_k, s_k, \alpha) \lambda(\vec{p}, \sigma_p, s_p, \alpha) \lambda(\vec{q}, \sigma_q, s_q, \alpha) \right. \\ & \left. + \lambda(\vec{k}, \sigma_k, -s_k, \alpha) \lambda(\vec{p}, \sigma_p, -s_p, \alpha) \lambda(\vec{q}, \sigma_q, -s_q, \alpha) \right), \quad (66) \end{aligned}$$

respectively. Explicit expression of the phase factor for $\{(\vec{k}, \vec{p}, \vec{q}); \vec{k} + \vec{p} + \vec{q} = \vec{0}\}$ is

$$e^{i\Psi\{\vec{k}, \vec{p}, \vec{q}\}} = \frac{\hat{z} \cdot (\mathbf{e}_n - i\sigma_p \mathbf{e}_b(\vec{p}))}{|\hat{z} \times \mathbf{e}_r(\vec{p})|} \frac{\hat{z} \cdot (\mathbf{e}_n - i\sigma_p \mathbf{e}_b(\vec{q}))}{|\hat{z} \times \mathbf{e}_r(\vec{q})|} \frac{\hat{z} \cdot (\mathbf{e}_n - i\sigma_p \mathbf{e}_b(\vec{k}))}{|\hat{z} \times \mathbf{e}_r(\vec{k})|},$$

where $\mathbf{e}_r(\vec{k}) := \vec{k}/|\vec{k}|$, $\mathbf{e}_n := (\vec{p} \times \vec{q})/|\vec{p} \times \vec{q}|$, $\mathbf{e}_b(\vec{k}) := \mathbf{e}_r(\vec{k}) \times \mathbf{e}_n$. Thus, the GEV representation of the Levi-Civita connection (16) is given by

$$\begin{aligned} \tilde{\nabla}_{\vec{\Phi}(\vec{p}, \sigma_p, s_p, \alpha)} \vec{\Phi}(\vec{q}, \sigma_q, s_q, \alpha) &= \sum_{\sigma_k, s_k} ((-\vec{p} - \vec{q}, \sigma_k, s_k \| \vec{p}, \sigma_p, s_p \| \vec{q}, \sigma_q, s_q)) \\ & \times \frac{\lambda(\vec{p}, \sigma_p, s_p, \alpha) - \lambda(\vec{q}, \sigma_q, s_q, \alpha) - \lambda(-\vec{p} - \vec{q}, \sigma_k, s_k, \alpha)}{2(1 + \lambda(-\vec{p} - \vec{q}, \sigma_k, s_k, \alpha)^2)} \vec{\Phi}(\vec{p} + \vec{q}, \sigma_k, s_k, \alpha; \vec{x}). \quad (67) \end{aligned}$$

Appendix 4. GEV mode representation of the HMHD sectional curvature and its Hall-term coefficient expansion

Substituting the explicit expression of the eigenvalues (54) and the integral of the triple product of the CHM (65) into Eq. (30) (i.e., Equations (66), (31), and (32)) and calculating with the aid of Mathematica, we can obtain the following GEV-mode sectional curvature between the modes (\vec{k}, σ_k, s_k) and (\vec{p}, σ_p, s_p) :

$$\begin{aligned} R_H(k, \sigma_k, s_k, p, \sigma_p, s_p, q, \alpha) &= \pi^2 k^2 \frac{(1 - \underline{p} - \underline{q})(1 + \underline{p} - \underline{q})(1 - \underline{p} + \underline{q})(1 + \underline{p} + \underline{q})}{16 \underline{p}^2 \underline{q}^2 (2 + 2\underline{p}^2 - \underline{q}^2)(1 + \lambda(\vec{k})^2)} \\ & \times \left\{ - (2 - 10\underline{p}^2 - 10\underline{p}^4 + 2\underline{p}^6 + \underline{q}^2 + 10\underline{p}^2 \underline{q}^2 + \underline{p}^4 \underline{q}^2 + 4\underline{q}^4 + 4\underline{p}^2 \underline{q}^4 - 3\underline{q}^6) \right. \\ & \quad + 2\sigma_k \sigma_p (1 + \lambda(\vec{k}) \lambda(\vec{p})) \underline{p} (2 + 4\underline{p}^2 + 2\underline{p}^4 - 9\underline{q}^2 - 9\underline{p}^2 \underline{q}^2 + 5\underline{q}^4) \\ & \quad + 2\lambda(\vec{k}) \lambda(\vec{p}) (2 + 2\underline{p}^6 + 2\underline{p}^2 + 2\underline{p}^4 - 5\underline{q}^2 - 4\underline{p}^2 \underline{q}^2 - 5\underline{p}^4 \underline{q}^2 + 4\underline{q}^4 + 4\underline{p}^2 \underline{q}^4 - \underline{q}^6) \\ & \quad - (2\pi\alpha\sigma_k k) \left[\lambda(\vec{k}) (2 + 2\underline{p}^4 + 4\underline{p}^6 - 7\underline{q}^2 - 11\underline{p}^2 \underline{q}^2 - 8\underline{p}^4 \underline{q}^2 + 3\underline{q}^4 + 4\underline{p}^2 \underline{q}^4) \right. \\ & \quad \left. + \lambda(\vec{p}) (2\underline{p}^2 + 2\underline{p}^4 - 2\underline{q}^2 - 5\underline{p}^2 \underline{q}^2 - 4\underline{p}^4 \underline{q}^2 + 3\underline{q}^4 + 4\underline{p}^2 \underline{q}^4 - \underline{q}^6) \right] \\ & \quad - (2\pi\alpha\sigma_p p) \left[\lambda(\vec{k}) (2\underline{p}^2 + 2\underline{p}^4 - 4\underline{q}^2 - 5\underline{p}^2 \underline{q}^2 - 2\underline{p}^4 \underline{q}^2 + 4\underline{q}^4 + 3\underline{p}^2 \underline{q}^4 - \underline{q}^6) \right. \\ & \quad \left. + \lambda(\vec{p}) (4 + 2\underline{p}^2 + 2\underline{p}^6 - 8\underline{q}^2 - 11\underline{p}^2 \underline{q}^2 - 7\underline{p}^4 \underline{q}^2 + 4\underline{q}^4 + 3\underline{p}^2 \underline{q}^4) \right] \\ & \quad + (2\pi\alpha\sigma_k k) (2\pi\alpha\sigma_p p) \left[\frac{\sigma_k \sigma_p}{\underline{p}} (2\underline{p}^2 + 4\underline{p}^4 + 2\underline{p}^6 - 2\underline{q}^2 - 7\underline{p}^2 \underline{q}^2 - 7\underline{p}^4 \underline{q}^2 \right. \\ & \quad \quad - 2\underline{p}^6 \underline{q}^2 - \underline{q}^4 - \underline{p}^2 \underline{q}^4 - \underline{p}^4 \underline{q}^4 + \underline{q}^6 + \underline{p}^2 \underline{q}^6) \\ & \quad \quad + 2(2\underline{p}^2 + 2\underline{p}^4 - 4\underline{q}^2 - 7\underline{p}^2 \underline{q}^2 - 4\underline{p}^4 \underline{q}^2 + 4\underline{q}^4 + 4\underline{p}^2 \underline{q}^4 - \underline{q}^6) \\ & \quad \quad \left. + \lambda(\vec{k}) \lambda(\vec{p}) ((1 - \underline{p})^2 - \underline{q}^2)((1 + \underline{p})^2 - \underline{q}^2)(2 + 2\underline{p}^2 - \underline{q}^2) \right] \left. \right\}. \quad (68) \end{aligned}$$

Hereafter $\underline{p} := p/k$, $\underline{q} := q/k$. The dependency on the linear-mode-branch parameters s_k and s_p is included in the eigenvalues $\lambda(\tilde{k})$ and $\lambda(\tilde{p})$. Integrating Equation (68) with respect to q , we can obtain the following shell-averaged curvature kernel for the HMHD system:

$$\begin{aligned}
& K_H(k, \sigma_k, s_k, p, \sigma_p, s_p, \alpha) \\
&= \frac{\pi^3 k^4 \underline{p}^3}{1 + \lambda(\tilde{k})^2} \left\{ -\frac{\underline{p}^3}{4} + \frac{7\underline{p}}{12} + \frac{7}{12\underline{p}} - \frac{1}{4\underline{p}^3} + \left(\frac{\underline{p}^4}{8} + \underline{p}^2 - \frac{9}{4} + \frac{1}{\underline{p}^2} + \frac{1}{8\underline{p}^4} \right) L(\underline{p}) \right. \\
&\quad \left. + \sigma_k \sigma_p (1 + \lambda(\tilde{k})\lambda(\tilde{p})) \left[-\frac{3}{2} \left(\underline{p}^2 + \frac{1}{\underline{p}^2} \right) + \frac{11}{3} + \frac{3}{4} \left(\underline{p}^3 - \underline{p} - \frac{1}{\underline{p}} + \frac{1}{\underline{p}^3} \right) L(\underline{p}) \right] \right. \\
&\quad \left. + \lambda(\tilde{k})\lambda(\tilde{p}) \left[-\frac{\underline{p}^3}{2} - \frac{7\underline{p}}{6} - \frac{7}{6\underline{p}} - \frac{1}{2\underline{p}^3} + \left(\frac{\underline{p}^4}{4} + \frac{\underline{p}^2}{2} - \frac{3}{2} + \frac{1}{2\underline{p}^2} + \frac{1}{4\underline{p}^4} \right) L(\underline{p}) \right] \right. \\
&\quad \left. + (\pi\alpha\sigma_k k) \left\{ \lambda(\tilde{p}) \left[\frac{\underline{p}}{3} + \frac{3}{\underline{p}} + \left(-\frac{3\underline{p}^2}{2} + 3 - \frac{3}{2\underline{p}^2} \right) L(\underline{p}) \right] \right. \right. \\
&\quad \left. \left. + \lambda(\tilde{k}) \left[2\underline{p}^3 - \frac{17\underline{p}}{6} - \frac{3}{\underline{p}} + \frac{1}{2\underline{p}^3} + \left(-\underline{p}^4 + \frac{7\underline{p}^2}{4} - \frac{3}{4} + \frac{1}{4\underline{p}^2} - \frac{1}{4\underline{p}^4} \right) L(\underline{p}) \right] \right\} \right. \\
&\quad \left. + (\pi\alpha\sigma_p p) \left\{ \lambda(\tilde{k}) \left[3\underline{p} + \frac{1}{3\underline{p}} + \left(-\frac{3\underline{p}^2}{2} + 3 - \frac{3}{2\underline{p}^2} \right) L(\underline{p}) \right] \right. \right. \\
&\quad \left. \left. + \lambda(\tilde{p}) \left[\frac{\underline{p}^3}{2} - 3\underline{p} - \frac{17}{6\underline{p}} + \frac{2}{\underline{p}^3} + \left(-\frac{\underline{p}^4}{4} + \frac{\underline{p}^2}{4} - \frac{3}{4} + \frac{7}{4\underline{p}^2} - \frac{1}{\underline{p}^4} \right) L(\underline{p}) \right] \right\} \right. \\
&\quad \left. + (\pi\alpha\sigma_k k)(\pi\alpha\sigma_p p) \left\{ -\frac{2\underline{p}}{3} - \frac{2}{3\underline{p}} + \left(3\underline{p}^2 - 6 + \frac{3}{\underline{p}^2} \right) L(\underline{p}) \right. \right. \\
&\quad \left. \left. + \lambda(\tilde{k})\lambda(\tilde{p}) \left[\underline{p}^3 - \frac{11\underline{p}}{3} - \frac{11}{3\underline{p}} + \frac{1}{\underline{p}^3} + \left(-\frac{\underline{p}^4}{2} + 2\underline{p}^2 - 3 + \frac{2}{\underline{p}^2} - \frac{1}{2\underline{p}^4} \right) L(\underline{p}) \right] \right. \right. \\
&\quad \left. \left. + \sigma_k \sigma_p \left[\frac{7\underline{p}^2}{3} + \frac{22}{3} + \frac{7}{3\underline{p}^2} + \left(\frac{3\underline{p}^3}{2} - \frac{3\underline{p}}{2} - \frac{3}{2\underline{p}} + \frac{3}{2\underline{p}^3} \right) L(\underline{p}) \right] \right\} \right\}. \tag{69}
\end{aligned}$$

Hereafter $L(\underline{p}) := \ln |(1 + \underline{p})/(1 - \underline{p})|$.

Because of its dependence on the eigenvalues $\lambda(\tilde{k})$ and $\lambda(\tilde{p})$, the GEV-mode sectional curvature is not a homogeneous expression with respect to the variables k , p , and q . However, they can be expanded in powers of $\pi\alpha k$ as follows:

$$R_H(k, \sigma_k, s_k, p, \sigma_p, s_p, q, \alpha) = (\pi k)^2 \sum_{n=0}^{\infty} (\pi\alpha k)^n \widehat{R}_H^{(n)}(\sigma_k, s_k, \underline{p}, \sigma_p, s_p, \underline{q}), \tag{70}$$

$$K_H(k, \sigma_k, s_k, p, \sigma_p, s_p, \alpha) = \pi^3 k^4 \sum_{n=0}^{\infty} (\pi\alpha k)^n \widehat{K}_H^{(n)}(\sigma_k, s_k, \underline{p}, \sigma_p, s_p), \tag{71}$$

where $\widehat{R}_H^{(n)}(\sigma_k, s_k, \underline{p}, \sigma_p, s_p, \underline{q})$ and $\widehat{K}_H^{(n)}(\sigma_k, s_k, \underline{p}, \sigma_p, s_p)$ are dimensionless, scale-independent, geometrical factor functions determined by the ratio of the wavenumber moduli \underline{p} and \underline{q} . The expansion parameter $\pi\alpha k$ measures the scale ratio of the observed motion scale to that of the ion skin depth.

MHD sectional curvature ($O(\alpha^0)$ terms in the HMHD sectional curvature)

As discussed in [14], the GEVs work as an orthogonal basis of the HMHD system and are the most suitable for avoiding problems with singularities that appear when the standard magnetohydrodynamic limit ($\alpha \rightarrow 0$) is considered. The leading-order terms $\pi^2 k^2 \widehat{R}_H^{(0)}$ and $\pi^3 k^4 \widehat{K}_H^{(0)}$ provide the stability information about the MHD dynamics. The MHD limit of the GEV-mode sectional curvature is a homogeneous expression of degree 2 with respect to k , p , and q and is given as follows:

$$\lim_{\alpha \rightarrow 0} R_H(k, \sigma_k, s_k, p, \sigma_p, s_p, q, \alpha) = (\pi k)^2 \widehat{R}_H^{(0)}(\underline{p}, \underline{q}, \sigma_k \sigma_p, s_k s_p),$$

where the geometric factor $\widehat{R}_H^{(0)}$ is given by

$$\begin{aligned} & \widehat{R}_H^{(0)}(\underline{p}, \underline{q}, \sigma_k \sigma_p, s_k s_p) \\ &= \frac{(1 - \underline{p} - \underline{q})(1 + \underline{p} - \underline{q})(1 - \underline{p} + \underline{q})(1 + \underline{p} + \underline{q})}{32 \underline{p}^2 \underline{q}^2 (2 + 2 \underline{p}^2 - \underline{q}^2)} \\ & \times \left[- \left(2 - 10 \underline{p}^2 - 10 \underline{p}^4 + 2 \underline{p}^6 + \underline{q}^2 + 10 \underline{p}^2 \underline{q}^2 + \underline{p}^4 \underline{q}^2 + 4 \underline{q}^4 + 4 \underline{p}^2 \underline{q}^4 - 3 \underline{q}^6 \right) \right. \\ & \quad + 2(\sigma_k \sigma_p + s_k s_p) \underline{p} (2 + 4 \underline{p}^2 + 2 \underline{p}^4 - 9 \underline{q}^2 - 9 \underline{p}^2 \underline{q}^2 + 5 \underline{q}^4) \\ & \quad \left. + 2 \sigma_k \sigma_p s_k s_p (2 + 2 \underline{p}^2 + 2 \underline{p}^4 + 2 \underline{p}^6 - 5 \underline{q}^2 - 4 \underline{p}^2 \underline{q}^2 - 5 \underline{p}^4 \underline{q}^2 + 4 \underline{q}^4 + 4 \underline{p}^2 \underline{q}^4 - \underline{q}^6) \right]. \quad (72) \end{aligned}$$

The shell-averaged curvature kernel associated with this MHD limit is given by

$$\lim_{\alpha \rightarrow 0} K_H(k, \sigma_k, s_k, p, \sigma_p, s_p, \alpha) = \pi^3 k^4 \widehat{K}_H^{(0)}(\underline{p}, \sigma_k \sigma_p, s_k s_p),$$

where the geometric factor $\widehat{K}_H^{(0)}$ is given by

$$\begin{aligned} & \widehat{K}_H^{(0)}(\underline{p}, \sigma_k \sigma_p, s_k s_p) \\ &= \frac{\underline{p}^3}{2} \left[- \frac{\underline{p}^3}{4} + \frac{7 \underline{p}}{12} + \frac{7}{12 \underline{p}} - \frac{1}{4 \underline{p}^3} + \left(\frac{\underline{p}^4}{8} + \underline{p}^2 - \frac{9}{4} + \frac{1}{\underline{p}^2} + \frac{1}{8 \underline{p}^4} \right) L(\underline{p}) \right. \\ & \quad + (\sigma_k \sigma_p + s_k s_p) \left(- \frac{3 \underline{p}^2}{2} + \frac{11}{3} - \frac{3}{2 \underline{p}^2} + \left(\frac{3 \underline{p}^3}{4} - \frac{3 \underline{p}}{4} - \frac{3}{4 \underline{p}} + \frac{3}{4 \underline{p}^3} \right) L(\underline{p}) \right) \\ & \quad \left. + \sigma_k \sigma_p s_k s_p \left(- \frac{\underline{p}^3}{2} - \frac{7 \underline{p}}{6} - \frac{7}{6 \underline{p}} - \frac{1}{2 \underline{p}^3} + \left(\frac{\underline{p}^4}{4} + \frac{\underline{p}^2}{2} - \frac{3}{2} + \frac{1}{2 \underline{p}^2} + \frac{1}{4 \underline{p}^4} \right) L(\underline{p}) \right) \right]. \quad (73) \end{aligned}$$

The helicity and linear-mode-branch parameters appear as the products $\sigma_k \sigma_p$ and $s_k s_p$, which implies that, for example, the stability feature of the interactions between the ion cyclotron branch modes is the same as those between the whistler branch modes, i.e., the stability features are invariant under linear-mode-branch exchange.

$O(\alpha^1)$ terms in the HMHD sectional curvature

The lowest order of the Hall term effect can be expressed as follows:

$$\alpha \lim_{\alpha \rightarrow 0} \frac{\partial}{\partial \alpha} R_H(k, \sigma_k, s_k, p, \sigma_p, s_p, q, \alpha) = \alpha \pi^3 k^3 \widehat{R}_H^{(1)}(\underline{p}, \underline{q}, \sigma_k \sigma_p, s_k, s_p), \quad (74)$$

where the geometric factor $\widehat{R}_H^{(1)}$ is given by

$$\begin{aligned} & \widehat{R}_H^{(1)}(\underline{p}, \underline{q}, \sigma_k \sigma_p, s_k, s_p) \\ &= -\frac{(1 - \underline{p} - \underline{q})(1 + \underline{p} - \underline{q})(1 - \underline{p} + \underline{q})(1 + \underline{p} + \underline{q})}{32\underline{p}^2\underline{q}^2(2 + 2\underline{p}^2 - \underline{q}^2)} \\ & \times \left[2\sigma_k \sigma_p s_k \underline{p} (6\underline{p}^2 + 4\underline{p}^4 - 2\underline{p}^6 - 12\underline{q}^2 - 15\underline{p}^2\underline{q}^2 + \underline{p}^4\underline{q}^2 + 9\underline{q}^4 + 2\underline{p}^2\underline{q}^4 - \underline{q}^6) \right. \\ & \quad + 4\sigma_k \sigma_p s_p (2\underline{p}^2 + 2\underline{p}^4 - 2\underline{q}^2 - 5\underline{p}^2\underline{q}^2 - 4\underline{p}^4\underline{q}^2 + 3\underline{q}^4 + 4\underline{p}^2\underline{q}^4 - \underline{q}^6) \\ & \quad + s_k (2 + 6\underline{p}^2 + 6\underline{p}^4 + 2\underline{p}^6 - 15\underline{q}^2 - 14\underline{p}^2\underline{q}^2 + \underline{p}^4\underline{q}^2 + 2\underline{q}^4 - 6\underline{p}^2\underline{q}^4 + 3\underline{q}^6) \\ & \quad \left. + 2s_p \underline{p} (4 + 2\underline{p}^2 + 2\underline{p}^6 - 8\underline{q}^2 - 11\underline{p}^2\underline{q}^2 - 7\underline{p}^4\underline{q}^2 + 4\underline{q}^4 + 3\underline{p}^2\underline{q}^4) \right]. \end{aligned} \quad (75)$$

The associated shell-averaged sectional curvature is given by

$$\alpha \lim_{\alpha \rightarrow 0} \frac{\partial}{\partial \alpha} K_H(k, \sigma_k, s_k, p, \sigma_p, s_p, q, \alpha) = \alpha \pi^4 k^5 \widehat{K}_H^{(1)}(\underline{p}, \sigma_k \sigma_p, s_k, s_p),$$

where the geometric factor $\widehat{K}_H^{(1)}$ is given by

$$\begin{aligned} & \widehat{K}_H^{(1)}(\underline{p}, \sigma_k \sigma_p, s_k, s_p) \\ &= \frac{\underline{p}^3}{2} \left\{ s_k \left[\left(\frac{3\underline{p}^3}{4} + \frac{3}{4\underline{p}^3} + \frac{\underline{p}}{4} - \frac{61}{12\underline{p}} \right) + \left(-\frac{3\underline{p}^4}{8} - \frac{3}{8\underline{p}^4} + \frac{3}{4} \right) L(\underline{p}) \right] \right. \\ & \quad + s_k \sigma_k \sigma_p \left[\left(-\frac{\underline{p}^4}{2} + \frac{10\underline{p}^2}{3} + \frac{1}{\underline{p}^2} - \frac{9}{2} \right) + \left(\frac{\underline{p}^5}{4} - \frac{7\underline{p}^3}{4} - \frac{1}{2\underline{p}^3} + \frac{9\underline{p}}{4} - \frac{1}{4\underline{p}} \right) L(\underline{p}) \right] \\ & \quad + s_p \left[\left(\frac{\underline{p}^4}{2} - 3\underline{p}^2 + \frac{2}{\underline{p}^2} - \frac{17}{6} \right) + \left(-\frac{\underline{p}^5}{4} + \frac{\underline{p}^3}{4} - \frac{1}{\underline{p}^3} - \frac{3\underline{p}}{4} + \frac{7}{4\underline{p}} \right) L(\underline{p}) \right] \\ & \quad \left. + s_p \sigma_k \sigma_p \left[\left(\frac{\underline{p}}{3} + \frac{3}{\underline{p}} \right) + \left(-\frac{3\underline{p}^2}{2} - \frac{3}{2\underline{p}^2} + 3 \right) L(\underline{p}) \right] \right\}. \end{aligned} \quad (76)$$

Appendix 5. CHW mode representation of the Euler sectional curvature

For comparison with the HMHD case, we examine the HD case, i.e., the case wherein the magnetic field is absent. As was discussed in [25], the dissipationless, incompressible HD, MHD, and HMHD systems have a common mathematical structure. The Riemannian metric and the Lie bracket are given by

$$\langle \mathbf{u}_1 | \mathbf{u}_2 \rangle := \int \mathbf{u}_1 \cdot \mathbf{u}_2 d^3 \vec{x}, \quad [\mathbf{u}_1, \mathbf{u}_2] = \nabla \times (\mathbf{u}_1 \times \mathbf{u}_2), \quad (77)$$

respectively. The helicity-based, particle-relabeling operator of the HD system is the curl operator, and its eigenfunctions are given by the CHWs. The values of the Riemannian metric and the Lie bracket, which correspond to Equations (56) and (64) in the HMHD case, are given by

$$\left\langle \overline{\phi(\vec{k}, \sigma_k)} \middle| \phi(\vec{p}, \sigma_p) \right\rangle = \delta_{-\vec{k}, \vec{p}}^3 \delta_{\sigma_k, \sigma_p}, \quad (78)$$

$$\left\langle \overline{\phi(\vec{k}, \sigma_k)} \middle| [\phi(\vec{p}, \sigma_p), \phi(\vec{q}, \sigma_q)] \right\rangle = \sigma_k k(\vec{k}, \sigma_k | \vec{p}, \sigma_p | \vec{q}, \sigma_q), \quad (79)$$

respectively, where the three-mode parenthesis symbol $(\vec{k}, \sigma_k | \vec{p}, \sigma_p | \vec{q}, \sigma_q)$ is defined by Eq. (65). The connection that satisfies the same three physical conditions discussed in section 2.2 is given by

$$\tilde{\nabla}_{\phi(\vec{p}, \sigma_p)} \phi(\vec{q}, \sigma_q) = \frac{1}{2} \sum_{\sigma_k}^{\vec{k} + \vec{p} + \vec{q} = \vec{0}} (\vec{k}, \sigma_k | \vec{p}, \sigma_p | \vec{q}, \sigma_q) (\sigma_p p - \sigma_q q - \sigma_k k) \phi(\vec{p} + \vec{q}, \sigma_k). \quad (80)$$

The geodesic equation corresponding to this connection is

$$\left(\frac{\partial}{\partial t} + \tilde{\nabla}_{\vec{v}} \right) \vec{V} = \frac{\partial \mathbf{u}}{\partial t} + \left((\mathbf{u} \cdot \nabla) \mathbf{u} \right)_S = 0. \quad (81)$$

The CHW-mode sectional curvature, which is the Euler counterpart of Eq. (68), becomes $R_E(k, \sigma_k, p, \sigma_p, q) = (\pi k)^2 \hat{R}_H(\underline{p}, \underline{q})$, where $\hat{R}_H(\underline{p}, \underline{q})$ is the geometric (i.e. $|\vec{k}|$ -independent) factor given by

$$\hat{R}_H(\underline{p}, \underline{q}) = - \frac{(1 - \underline{p} - \underline{q})^2 (1 + \underline{p} - \underline{q})^2 (1 - \underline{p} + \underline{q})^2 (1 + \underline{p} + \underline{q})^2}{16 \underline{p}^2 \underline{q}^2}. \quad (82)$$

The corresponding shell-averaged curvature kernel (cf. Equation (35)) is given by $K_E(k, \sigma_k, p, \sigma_p, \alpha) = \pi^3 k^4 \hat{K}_E(\underline{p})$, where $\hat{K}_E(\underline{p})$ is the geometric factor given by

$$\hat{K}_E(\underline{p}) = \underline{p}^3 \left[\frac{\underline{p}^3}{4} - \frac{11\underline{p}}{12} - \frac{11}{12\underline{p}} + \frac{1}{4\underline{p}^3} - \left(\frac{\underline{p}^4}{8} - \frac{\underline{p}^2}{2} + \frac{3}{4} - \frac{1}{2\underline{p}^2} + \frac{1}{8\underline{p}^4} \right) L(\underline{p}) \right]. \quad (83)$$

It is interesting that the obtained CHM-mode sectional curvature does not have a helicity parameter even though one is taken into account in the derivation.

Appendix 6. Physical picture of the nonlocal interaction in the MHD case

For the mode interaction between the observed perturbation mode $(\mathbf{u}_k, \mathbf{b}_k)$ and the reference flow mode $(\mathbf{u}_p, \mathbf{b}_p)$, which is spatially large compared with the perturbation ($p \ll k$), the evolution equation (1) can be approximated as follows:

$$\begin{cases} (\partial_t + \mathbf{u}_p \cdot \nabla) \mathbf{u}_k = (\mathbf{b}_p \cdot \nabla) \mathbf{b}_k, \\ (\partial_t + \mathbf{u}_p \cdot \nabla) \mathbf{b}_k = (\mathbf{b}_p \cdot \nabla) \mathbf{u}_k. \end{cases}$$

This equation has solutions that are Alfvén waves propagating in a frame moving with velocity \mathbf{u}_p . Hence, the characteristic time scale is given by $\mathbf{b}_p \cdot \vec{k}$ or $\mathbf{v}_p \cdot \vec{k}$. Their values are $\mathbf{u}_p \cdot \vec{k} = \hat{u}_p k \sin \theta$, $\mathbf{b}_p \cdot \vec{k} = \hat{b}_p k \sin \theta$, respectively, where θ is the angle between \vec{k} and \vec{p} , because the velocity and magnetic fields are solenoidal ($\mathbf{u}_p, \mathbf{b}_p \perp \vec{p}$). Thus, the square of the characteristic time scale is given by $|\mathbf{u}_p \cdot \vec{k}|^2 = |\mathbf{b}_p \cdot \vec{k}|^2 = \frac{1}{2} Q(p) k^2 \sin^2 \theta$. Integrating this equation over a constant $|\vec{p}|$ shell, we can obtain the net time scale factor arising from the Alfvén waves on a constant $|\vec{p}|$ shell as $\frac{1}{2} \int \int Q(p) k^2 p^2 \sin^3 \theta d\theta d\phi = \frac{4}{3} \pi k^2 p^2 Q(p)$. As mentioned in the section 4.2, the geometric factor of the shell-averaged curvature kernel for the MHD system behaved as $K_H^{(0)}(k, p) = \frac{4}{3} \pi^3 k^4 p^2 + o(p^2)$ for sufficiently small wave numbers $p \ll k$. Thus, the contribution of small wavenumber component (i.e. the large-scale plasma motion) to the sectional curvature $K_H^{(0)}(p) Q(p) = \frac{4}{3} \pi^3 k^4 p^2 Q(p)$

is conjectured to be due to the propagation of the Alfvén waves. The fact that the sectional curvature was positive is consistent with the oscillatory, non-growing motion of the Alfvén waves (see section 3.3).

Reference

- [1] V. I. Arnold. Sur la géométrie différentielle des groupes de lie de dimension infinie et ses applications à l'hydrodynamique des fluides parfaits. *Annales de l'institut Fourier*, 16:319–361, 1966.
- [2] V. I. Arnold and B. A. Khesin. *Topological methods in hydrodynamics*. Springer-Verlag, New York, 1998.
- [3] J. E. Marsden and T. Ratiu. *Introduction to mechanics and symmetry: a basic exposition of classical mechanical systems*. Springer-Verlag, New York, 1999.
- [4] V. I. Arnold. *Mathematical methods of classical mechanics*. Springer-Verlag, New York, 1989.
- [5] F. Nakamura, Y. Hattori, and T. Kambe. Geodesics and curvature of a group of diffeomorphisms and motion of an ideal fluid. *Journal of Physics A: Mathematical and General*, 25:L45, 1992.
- [6] A. M. Lukatskii. On the curvature of the group of measure-preserving diffeomorphisms of an n-dimensional torus. *Russian Mathematical Surveys*, 36:179–180, 1981.
- [7] K. Ohkitani. Numerical study on the incompressible Euler equations as a Hamiltonian system: Sectional curvature and Jacobi field. *Physics of Fluids*, 22:057101, 2010.
- [8] P. Rouchon. Jacobi equation, riemannian curvature and the motion of a perfect incompressible fluid. *European Journal of Mechanics, B/Fluids*, 11:317–336, 1992.
- [9] V. Zeitlin and T. Kambe. Two-dimensional ideal magnetohydrodynamics and differential geometry. *Journal of Physics A: Mathematical General*, 26:5025–5031, 1993.
- [10] Y. Hattori. Differential-geometric structures of ideal magnetohydrodynamics and plasma instabilities. *J. Math-for-industry*, 3:119–123, 2011.
- [11] C. Vizman. Geodesic equations on diffeomorphism groups. *Symmetry, Integrability and Geometry: Methods and Applications*, 4:030, 2008.
- [12] C. Vizman. Geodesics and curvature of semidirect product groups. *Rendiconti del Circolo Matematico di Palermo, Serie II, Supplemento*, 66:199–206, 2001.
- [13] K. Araki. Differential-geometrical approach to the dynamics of dissipationless incompressible hall magnetohydrodynamics: I. lagrangian mechanics on semidirect product of two volume preserving diffeomorphisms and conservation laws. *Journal of Physics A: Mathematical and Theoretical*, 48:175501, 2015.
- [14] K. Araki. Helicity-based particle-relabeling operator and normal mode expansion of the dissipationless incompressible hall magnetohydrodynamics. *Physical Review E*, 92:063106, 2015.
- [15] S. Kobayashi and K. Nomizu. *Foundations of differential geometry. Volume I*. Interscience tracts in pure and applied mathematics. Interscience, New-York, 1963.
- [16] M. J. Lighthill. Studies on magneto-hydrodynamic waves and other anisotropic wave motions. *Philosophical Transactions of the Royal Society of London Series A*, 252:397–430, 1960.
- [17] D. D. Holm. Hall magnetohydrodynamics: Conservation laws and lyapunov stability. *Phys. Fluids*, 30:1310–1322, 1987.
- [18] F. Sagraoui, G. Belmont, and L. Rezeau. Hamiltonian canonical formulation of hall-magnetohydrodynamics: Toward an application to weak turbulence theory. *Phys. Plasmas*, 10:1325, 2003.
- [19] M. Hirota, Z. Yoshida, and E. Hameiri. Variational principle for linear stability of flowing plasmas in hall magnetohydrodynamics. *Phys. Plasmas*, 13:022107, 2006.
- [20] Z. Yoshida and E. Hameiri. Canonical hamiltonian mechanics of hall magnetohydrodynamics and its limit to ideal magnetohydrodynamics. *J. Phys. A: Math. Theor.*, 46:335502, 2013.

- [21] S. Galtier. Wave turbulence in incompressible hall magnetohydrodynamics. *Journal of Plasma Physics*, 72:721–769, 2006.
- [22] P. D. Mininni, A. Alexakis, and A. Pouquet. Energy transfer in Hall-MHD turbulence: cascades, backscatter, and dynamo action. *J. Plasma Phys.*, 73:377–401, 2007.
- [23] H. Miura and K. Araki. Structure transitions induced by the hall term in homogeneous and isotropic magnetohydrodynamic turbulence. *Phys. Plasmas*, 21:072313, 2015.
- [24] M. Yamada and Y. Saiki. Chaotic properties of a fully developed model turbulence. *Nonlinear Processes in Geophysics*, 14:631–640, September 2007.
- [25] K. Araki. Particle relabeling symmetry, generalized vorticity, and normal-mode expansion of ideal, incompressible fluids and plasmas in three-dimensional space. *ArXiv e-prints*, 1601.05477, 2016.
- [26] S. M. Mahajan and Z. Yoshida. Double curl beltrami flow: Diamagnetic structures. *Phys. Rev. Lett.*, 81:4863–4866, Nov 1998.
- [27] K. Araki. A comprehensive view of lagrangian invariants of hydrodynamics, ideal and hall magnetohydrodynamics on three-dimensional riemannian manifold. *J. Math-for-industry*, 1:139–147, 2009.
- [28] A. V. Tur and V. V. Yanovsky. Invariants in dissipationless hydrodynamic media. *J. Fluid Mech.*, 248:67–106, 1993.
- [29] S. I. Goldberg. *Curvature and homology*. Academic Press, New York, 1962.
- [30] F. Waleffe. The nature of triad interactions in homogeneous turbulence. *Physics of Fluids A*, 4:350–363, 1992.
- [31] K. Araki and H. Miura. Energy transfer between ion cyclotron and whistler modes in hall magnetohydrodynamic turbulence. 24th International Congress of Theoretical and Applied Mathematics, 2016.